Exact and leading order radiative effects in semi-inclusive deep inelastic scattering

Igor Akushevich[*] and Stanislav Srednyak[†]

Physics Department, Duke University, Durham, North Carolina 27708, USA

Alexander Ilyichev[‡]

Belorussian State University, Minsk, 220030, Belarus and Institute for Nuclear Problems,
Belorussian State University, Minsk, 220006, Belarus

Radiative effects in semi-inclusive hadron leptoproduction of unpolarized particles are calculated within the leading order approximation. The contributions of the infrared-free sum of the effects of real and virtual photon emission as well as the contribution of the exclusive radiative tail are considered. It is demonstrated how the obtained formulas in the leading log approximation can be obtained using the standard approach of the leading log approximation as well as from the exact expressions for the radiative correction of the lowest order. The method of the electron structure function is used to calculate the higher order corrections. The results are analytically compared to the results obtained by other groups. Numeric illustrations are given in the kinematics of the modern experiments at Jefferson Laboratory.

I. INTRODUCTION

Modern experiments on semi-inclusive deep inelastic in ep-scattering (SIDIS) provide information about the multidimensional structure of the nucleon that is not accessible in inclusive DIS. Current and planned experiments in several laboratories, such as JLab, BNL, and CERN have precision that necessitates consideration and implementation of radiative corrections (RC). The main contribution to RC in SIDIS comes from the emission of real photons by the initial and final electrons. The radiated photon is not detected in the detector by the design of SIDIS measurements; therefore, the observed cross sections have to be integrated with respect to the phase space of the radiated photons. The integration in the soft photon region (i.e., when the photon energy is small) cannot be completed because of the infrared divergence that cancels in the sum with the contributions of loop diagrams (e.g., the vertex function in the lowest order). A special procedure of covariant extraction and cancellation of the infrared divergence developed by Bardin and Shumeiko [1] is usually applied. An attractive property of the approach is the lack of simplifying assumptions that

make the obtained formulas nonexact and dependent on artificial parameters, such as Δ, minimal photon energy in the Mo and Tsai formalism [2]. An additional contribution to RC is the radiative tail from the exclusive peak (or exclusive radiative tail) that is characterized by the radiated photon and a single hadron in the unobserved hadronic state. This process contributes to RC to SIDIS when the invariant mass of the radiated photon and unobserved hadron equals the mass of the unobserved hadronic state in the base SIDIS process. The complete set of Feynman diagrams that are needed to be considered to calculate the lowest order RC is shown in Fig. 1.

The original formalism for RC in SIDIS in the simple quark-parton model was suggested in [3,4], which was later implemented in POLRAD 2.0 as a patch SIRAD [5]. The formulas allowed for calculating RC for the three-dimensional SIDIS cross section averaged over polar angle and transverse momentum of the final hadron. The formalism was then generalized in [6] to allow the calculation for the five-dimensional SIDIS cross section in the scattering of unpolarized particles. The exclusive radiative tail was first shown calculated (to the best of our knowledge) in [7].

The general calculation of RC for polarized particles was recently performed in [8], and the code for numeric calculation of RC to the SIDIS cross section of electron scattering arbitrary polarized particles was created. This calculation provides the so-called exact computation of RC. By "exactly" calculated RC we understand the estimation of the lowest order RC contribution with any predetermined accuracy. The structure of the dependence on the electron mass in the RC cross section is

[*]igor.akushevich@duke.edu
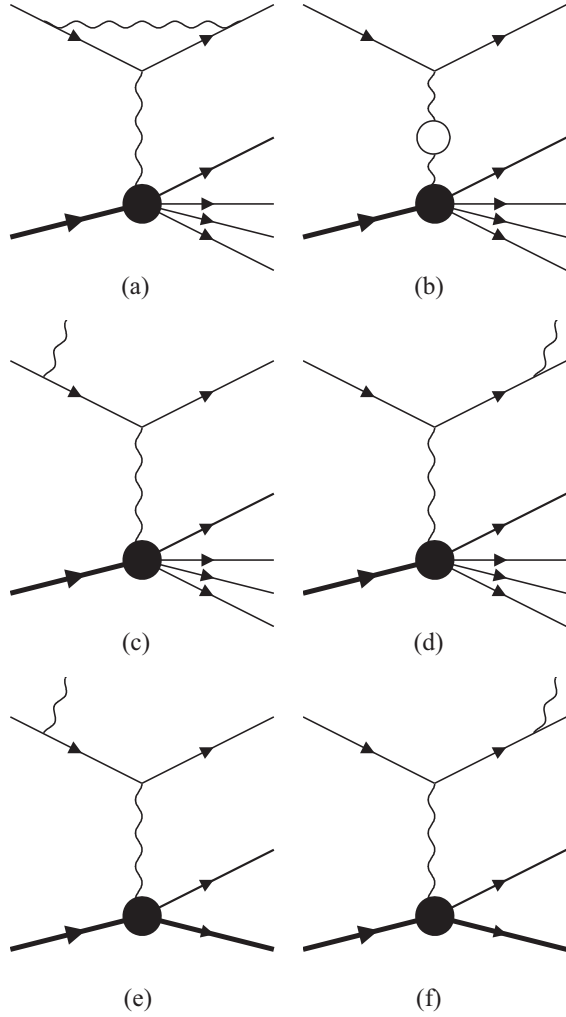[†]stan.sredn@gmail.com
[‡]ily@hep.by

FIG. 1. Feynman graphs (a)–(d) for the contributions to the lowest order RC from semi-inclusive processes and (e) and (f) for the exclusive radiative tail.

$$\sigma_{\mathrm{RC}} = A l_m + B + O(m^2/Q^2), \qquad (1)$$

where $l_m = \log(Q^2/m^2)$ and A and B do not depend on the electron mass m. If only A is kept in the formulas for RC, this is the leading log approximation that evaluates the contributions of photons radiated collinearly to the initial or final electrons. If both contributions are kept (i.e., contained A and B), this is the calculation with the next-to-leading accuracy, practically equivalent to the exact calculation.

The leading log approximation for the calculation of RC was first suggested in QCD by Dokshitzer [9], Gribov-Lipatov [10], and Altarelli-Parisi [11]. How the approximation can be applied for the lepton current was demonstrated by De Rújula, Petronzio, and Savoy-Navarro [12]. The QCD-based approach was adapted for real photon emission at the first order $\mathcal{O}(\alpha l_m)$ by Blümlein [13], second order $\mathcal{O}((\alpha l_m)^2)$ by Kripfganz, Mohring, and Spiesberger [14], third order $\mathcal{O}((\alpha l_m)^3)$ by Skrzypek [15], and second order

subleading term $\mathcal{O}(\alpha^2 l_m)$ and fifth order $\mathcal{O}((\alpha l_m)^5)$ by Blümlein and Kawamura in [16] and [17], respectively.

On the other side the leading log formulas can also be extracted from the exact formulas. Traditionally, such a calculation represents a reasonable step in obtaining the formulas for RC [e.g., exact [18] and leading log [19] formulas for the RC to deep virtual Compton scattering cross section] because the obtained formulas are compact and provide an actually leading contribution of RC to the cross section.

At last, a complete resummation of the leading log terms in all orders with respect to α has been performed by Kuraev and Fadin in their seminal work [20]. In collaboration with Merenkov they showed how subleading terms in all order of α have to be accounted for in their resummation scheme [21]. Such a scheme was applied for polarized DIS [22,23] and for initial state QED radiation aspects in data analyses of future e^+e^- colliders [24].

Thus, three approaches to extract the leading log contributions for the SIDIS cross section (i.e., to calculate A) include the following: (i) extract the poles that correspond to radiation collinear to initial and final electrons, integrate over angles, and find the factorized form traditional for leading log calculations; (ii) use our exact formulas, collect all terms that result in a leading log after integration over photon angles, combine them into the final expression; and (iii) use the method of the electron structure functions [22]. All these approaches are applied and discussed in our paper. Recently, a new factorized approach to SIDIS was suggested which treats QED and QCD radiation equally [25]. The approach is similar to the methods of electron structure functions, and the results obtained provide analytical comparison with our formulas.

We introduce the set of kinematical variables and calculate the Born cross section in Sec. II. The calculations of RC using the three approaches are presented in Sec. III. Both SIDIS RC and the contribution of the exclusive radiative tail are studied in the leading and next-to-leading approximations. Numeric estimates in the kinematical conditions of modern experiments at JLab are presented in Sec. V. The leading, next-to-leading, as well as higher order corrections obtained using the electron structure functions are numerically compared. Section VI contains discussion of the obtained results, computational tricks, role of the results in data analyses of SIDIS experiments, and comparison with the results obtained in [25].

II. BORN CROSS SECTION

The SIDIS process

$$l(k_1) + n(p) \rightarrow l(k_2) + h(p_h) + x(p_x) \qquad (2)$$

$(k_1^2 = k_2^2 = m^2, \quad p^2 = M^2, \quad p_h^2 = m_h^2)$ is traditionally described by the set of kinematical variables

$$x = -\frac{q^2}{2qp}, \quad y = \frac{qp}{k_1 p}, \quad z = \frac{p_h p}{pq}, \quad t = (q - p_h)^2, \quad \phi_h.$$

$$(3)$$

Here $q = k_1 - k_2$, ϕ_h is the angle between $(\mathbf{k_1}, \mathbf{k_2})$ and $(\mathbf{q}, \mathbf{p_h})$ planes.

In most analyses the transverse momentum of the detected hadron p_t or its square is used instead of t. Their relationship is presented below in Eq. (6). Formally, the p_t is the orthogonal part of the three-vector $\mathbf{p_h}$ with respect to $\mathbf{q}$ in the lab frame.

The set of additional quantities are used to describe the Born cross section. So, the invariants dependent on lepton momenta are identical to those used in DIS:

$$S = 2pk_1, \quad Q^2 = -q^2, \quad X = 2pk_2, \quad S_x = S - X,$$
$$\lambda_S = S^2 - 4m^2 M^2, \quad \lambda_X = X^2 - 4m^2 M^2,$$
$$S_p = S + X, \quad \lambda_Y = S_x^2 + 4M^2 Q^2,$$
$$\lambda_1 = Q^2(SX - M^2 Q^2) - m^2 \lambda_Y,$$
$$W^2 = (p + q)^2 = S_x - Q^2 + M^2, \quad (4)$$

whereas involvement of the detected hadron generates a set of new invariants:

$$V_{1,2} = 2k_{1,2} p_h, \quad V_+ = \frac{1}{2}(V_1 + V_2),$$
$$V_- = \frac{1}{2}(V_1 - V_2) = \frac{1}{2}(m_h^2 - Q^2 - t),$$
$$S' = 2k_1(p + q - p_h) = S - Q^2 - V_1,$$
$$X' = 2k_2(p + q - p_h) = X + Q^2 - V_2,$$
$$p_x^2 = (p + q - p_h)^2 = M^2 + t + (1 - z)S_x,$$
$$\lambda_S' = S'^2 - 4m^2 p_x^2, \quad \lambda_X' = X'^2 - 4m^2 p_x^2. \quad (5)$$

Noninvariant variables, such as the energy p_{h0}, longitudinal p_l, and transverse p_t (k_t) three-momenta of the detected hadron (the incoming or scattering lepton) with respect to the virtual photon direction, in the target rest frame are expressed in terms of the above invariants:

$$p_{h0} = \frac{zS_x}{2M},$$
$$p_l = \frac{zS_x^2 - 4M^2 V_-}{2M\sqrt{\lambda_Y}} = \frac{zS_x^2 + 2M^2(t + Q^2 - m_h^2)}{2M\sqrt{\lambda_Y}},$$
$$p_t = \sqrt{p_{h0}^2 - p_l^2 - m_h^2},$$
$$k_t = \sqrt{\frac{\lambda_1}{\lambda_Y}}. \quad (6)$$

As a result the quantities $V_{1,2}$ can be written through $\cos\phi_h$ and other variables defined in Eqs. (3)–(6) as
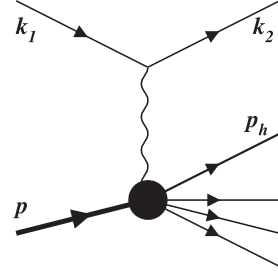

FIG. 2. Feynman graph for the lowest order SIDIS.

$$V_1 = p_{h0}\frac{S}{M} - \frac{p_l(SS_x + 2M^2 Q^2)}{M\sqrt{\lambda_Y}} - 2p_t k_t \cos\phi_h,$$
$$V_2 = p_{h0}\frac{X}{M} - \frac{p_l(XS_x - 2M^2 Q^2)}{M\sqrt{\lambda_Y}} - 2p_t k_t \cos\phi_h. \quad (7)$$

From the other side

$$\cos\phi_h = \frac{S_p S_x(zQ^2 + V_-) - \lambda_Y V_+}{2p_t\sqrt{\lambda_Y \lambda_1}}. \quad (8)$$

The lowest order QED (Born) contribution to SIDIS is presented by the Feynman graph in Fig. 2. The cross section for this process reads

$$d\sigma_B = \frac{(4\pi\alpha)^2}{2SQ^4} W_{\mu\nu}(q, p, p_h) L_B^{\mu\nu} d\Gamma_B, \quad (9)$$

where the phase space is parametrized as

$$d\Gamma_B = (2\pi)^4 \frac{d^3 k_2}{(2\pi)^3 2k_{20}} \frac{d^3 p_h}{(2\pi)^3 2p_{h0}}$$
$$= \frac{1}{4(2\pi)} \frac{S_x dx dy}{2} \frac{S_x dz dp_t^2 d\phi_h}{4M p_l}. \quad (10)$$

The leptonic tensor can be presented as

$$L_B^{\mu\nu} = \frac{1}{2}\text{Tr}[(\hat{k}_2 + m)\gamma_\mu(\hat{k}_1 + m)\gamma_\nu]$$
$$= 2k_1^\mu k_2^\nu + 2k_2^\mu k_1^\nu - Q^2 g^{\mu\nu}. \quad (11)$$

According to [8] the hadronic tensor can be written in the covariant form

$$W_{\mu\nu}(q, p, p_h) = \sum_{i=1}^{4} w_{\mu\nu}^i(q, p, p_h)\mathcal{H}_i$$
$$= -g_{\mu\nu}^\perp \mathcal{H}_1 + p_\mu^\perp p_\nu^\perp \mathcal{H}_2 + p_{h\mu}^\perp p_{h\nu}^\perp \mathcal{H}_3$$
$$+ (p_\mu^\perp p_{h\nu}^\perp + p_{h\mu}^\perp p_\nu^\perp)\mathcal{H}_4. \quad (12)$$

Here $g_{\mu\nu}^{\perp} = g_{\mu\nu} - q_\mu q_\nu/q^2$, for any four-vector $a_\mu^{\perp} = a_\mu + aq q_\mu/Q^2$.

Finally, we find the Born contribution in the form

$$
\begin{aligned}
&\sigma_B(S, Q^2, x, z, p_t, \cos\phi_h) \\
&\equiv \frac{d\sigma_B}{dx\,dy\,dz\,dp_t^2\,d\phi_h} \\
&= \frac{\pi\alpha^2 S_x^2}{4MQ^4 p_l S} \sum_{i=1}^{4} \theta_i^B(S, x, y, z, p_t, \cos\phi_h) \\
&\quad \times \mathcal{H}_i(Q^2, x, z, p_t),
\end{aligned}
\tag{13}
$$

where $\theta_i^B = L_B^{\mu\nu} w_{\mu\nu}^i / 2$,

$$
\begin{aligned}
\theta_1^B &= Q^2, \\
\theta_2^B &= (SX - M^2 Q^2)/2, \\
\theta_3^B &= (V_1 V_2 - m_h^2 Q^2)/2, \\
\theta_4^B &= (SV_2 + XV_1 - zQ^2 S_x)/2.
\end{aligned}
\tag{14}
$$

The generalized structure functions can be expressed in terms of another set of the structure functions [26] $F_{UU,T}$, $F_{UU,L}$, $F_{UU}^{\cos\phi_h}$, and $F_{UU}^{\cos 2\phi_h}$:

$$
\begin{aligned}
\mathcal{H}_1 &= C_1[F_{UU,T} - F_{UU}^{\cos 2\phi_h}], \\
\mathcal{H}_2 &= \frac{4C_1}{\lambda_Y^2 p_t^2}\Big[\lambda_Y p_t^2 Q^2 F_{UU,L} + \lambda_3^2 S_x^2(F_{UU}^{\cos 2\phi_h} + F_{UU,T}) - \lambda_2\lambda_Y(F_{UU,T} - F_{UU}^{\cos 2\phi_h}) + 2S_x\lambda_3 p_t Q\sqrt{\lambda_Y}F_{UU}^{\cos\phi_h}\Big], \\
\mathcal{H}_3 &= \frac{2C_1}{p_t^2}F_{UU}^{\cos 2\phi_h}, \\
\mathcal{H}_4 &= -\frac{2C_1}{\lambda_Y p_t^2}[2\lambda_3 S_x F_{UU}^{\cos 2\phi_h} + p_t Q\sqrt{\lambda_Y}F_{UU}^{\cos\phi_h}],
\end{aligned}
\tag{15}
$$

where $C_1 = 4Mp_l(Q^2 + 2xM^2)/Q^4$, $\lambda_2 = V_-^2 + m_h^2 Q^2$, and $\lambda_3 = V_- + zQ^2$. The Born cross section (13) expressed in the terms of these structure functions has a rather simple structure,

$$
\sigma_B = \frac{\pi\alpha^2}{xQ^2}\frac{y}{1-\varepsilon}\left(1 + \frac{\gamma^2}{2x}\right)\left\{F_{UU,T} + \varepsilon F_{UU,L} + \sqrt{2\varepsilon(1+\varepsilon)}\cos\phi_h F_{UU}^{\cos\phi_h} + \varepsilon\cos 2\phi_h F_{UU}^{\cos 2\phi_h}\right\},
\tag{16}
$$

where $\gamma = 2Mx/Q$ and ε is the ratio of the longitudinal and transverse photon fluxes,

$$
\varepsilon = \frac{1 - y - \gamma^2 y^2/4}{1 - y + y^2/2 + \gamma^2 y^2/4}.
\tag{17}
$$

III. THREE APPROACHES FOR LEADING LOGARITHMIC EXTRACTION

The QED RC come from three principal contributions: loop diagrams [Figs. 1(a) and 1(b)]; emission of the unobserved real photon in semi-inclusive [Figs. 1(c) and 1(d)]; and exclusive [Figs. 1(e) and 1(f)] processes. The calculation of the loop diagrams involves the procedure of subtraction of the ultraviolet divergence which is based on the idea of the electric charge renormalization. After that the integral over the loop momentum still contains the infrared divergence that cancels in the sum with the contribution of the real photon emission in a semi-inclusive process. The contribution of the exclusive

radiative tail does not contain the infrared divergence because of kinematical restrictions and can be calculated separately from other contributions.

As it was mentioned in the Introduction there are three approaches to extracting leading log contributions. In this section we describe each of them.

A. Extraction of the collinear poles

The contribution of real photon emission

$$
l(k_1) + n(p) \rightarrow l(k_2) + h(p_h) + x(p_x) + \gamma(k)
\tag{18}
$$

$(k^2 = 0)$ from the lepton leg shown in Figs. 1(a) and 1(b) can be presented as a convolution of the leptonic tensor with the real photon emission whose structure is well-known:

$$L_R^{\mu\nu} = -\frac{1}{2}\text{Tr}[(\hat{k}_2 + m)\Gamma_R^{\mu\alpha}(\hat{k}_1 + m)\bar{\Gamma}_{R\alpha}^{\nu}],$$

$$\Gamma_R^{\mu\alpha} = \left(\frac{k_1^{\alpha}}{kk_1} - \frac{k_2^{\alpha}}{kk_2}\right)\gamma^{\mu} - \frac{\gamma^{\mu}\hat{k}\gamma^{\alpha}}{2kk_1} - \frac{\gamma^{\alpha}\hat{k}\gamma^{\mu}}{2kk_2},$$

$$\bar{\Gamma}_{R\alpha}^{\nu} = \gamma_0 \Gamma_{R\alpha}^{\nu\dagger}\gamma_0$$

$$= \left(\frac{k_{1\alpha}}{kk_1} - \frac{k_{2\alpha}}{kk_2}\right)\gamma^{\nu} - \frac{\gamma^{\nu}\hat{k}\gamma_{\alpha}}{2kk_2} - \frac{\gamma_{\alpha}\hat{k}\gamma^{\nu}}{2kk_1}, \quad (19)$$

and the hadronic tensor (12),

$$d\sigma^R = \frac{(4\pi\alpha)^3}{2S(q-k)^4}W_{\mu\nu}(q-k, p, p_h)L_R^{\mu\nu}d\Gamma_R, \quad (20)$$

where

$$d\Gamma_R = (2\pi)^4 \frac{d^3k}{(2\pi)^3 2k_0}\frac{d^3k_2}{(2\pi)^3 2k_{20}}\frac{d^3p_h}{(2\pi)^3 2p_{h0}}$$

$$= \frac{1}{8(2\pi)^4}\frac{SS_x dxdy}{2\sqrt{\lambda_S}}\frac{S_x dz dp_t^2 d\phi_h}{4Mp_l}\frac{d^3k}{k_0}. \quad (21)$$

Integration over the photon angles can result in the leading log term. For example,

$$\int \frac{d\Omega_k}{kk_1} = \frac{1}{E_\gamma}\int \frac{d\Omega_k}{E_1 - |\mathbf{k}_1|\cos\theta_\gamma}$$

$$= \frac{2\pi}{E_\gamma|\mathbf{k}_1|}\log\frac{E_1 + |\mathbf{k}_1|}{E_1 - |\mathbf{k}_1|} \approx \frac{2\pi}{E_\gamma E_1}\log\frac{4E_1^2}{m^2}. \quad (22)$$

Similarly, integration of the terms with $(kk_1)^{-2}$ results in

$$\int \frac{d\Omega_k}{(kk_1)^2} = \frac{1}{E_\gamma^2}\int \frac{d\Omega_k}{(E_1 - |\mathbf{k}_1|\cos\theta_\gamma)^2} \approx \frac{2\pi}{E_\gamma^2 E_1^2}\frac{2E_1}{m^2}. \quad (23)$$

Since the squared propagators appear with a factor of m^2, i.e., as $m^2/(kk_1)^2$ and $m^2/(kk_2)^2$, such terms do not result in the leading log terms. Thus, the procedure of extraction of the leading log term in the standard leading log approximation [12–14,19,27] contains the following steps. In each convolution of leptonic tensor $L_R^{\mu\nu}$ with the tensor structures $w_{\mu\nu}^i$ in the hadronic tensor, the electron mass can be neglected everywhere in the numerators. Then, the terms containing $1/kk_1$ and $1/kk_2$ have to be extracted, i.e., the convolutions have to be presented in the form of two terms that are historically known as s- and p-peaks

$$L_R^{\mu\nu} w_{\mu\nu}^i(q - k, p, p_h)\mathcal{H}_i(q - k)$$

$$= \frac{G_s^i(k, \ldots)\mathcal{H}_i(q - k)}{kk_1}$$

$$+ \frac{G_p^i(k, \ldots)\mathcal{H}_i(q - k)}{kk_2}. \quad (24)$$

We note that the convolutions can have the terms with $1/(kk_1kk_2)$ that can be decomposed as

$$\frac{1}{kk_1}\frac{1}{kk_2} = -\frac{1}{k(k_1 - k_2)}\frac{1}{kk_1} + \frac{1}{k(k_1 - k_2)}\frac{1}{kk_2}. \quad (25)$$

The term $k(k_1 - k_2)$ is regular (i.e., not equaling zero for any peak) and can be included with a respective $G_{s,p}^i(k, \ldots)$. Since $G_{s,p}^i$ are regular functions of the momentum k, this momentum (as well as all kinematical variables containing k) can be taken in the respective peaks in $G_{s,p}^i$ as well as in arguments of structure functions $\mathcal{H}_i$. The four arguments of structure functions $\mathcal{H}_i$ come from the four scalar products pq, pp_h, q^2, and qp_h. Only the vector q has to change if the photon is radiated $q \to q - k$. Therefore, we can write for (24)

$$\frac{L_R^{\mu\nu} w_{\mu\nu}^i(q - k, p, p_h)\mathcal{H}_i(q - k)}{(q - k)^2}$$

$$= \frac{G_s^i(k_s, \ldots)\mathcal{H}_i(q - k_s)}{(q - k_s)^2 kk_1} + \frac{G_p^i(k_p, \ldots)\mathcal{H}_i(q - k_p)}{(q - k_p)^2 kk_2}. \quad (26)$$

In the standard leading log approximation the substitutions of the vector k in the s- and p-peaks are performed by the introduction of dimensionless variables z_1 and z_2 that reflect the remaining degree of freedom, i.e., photon energy, as follows $k \to k_{s,p}$ where

$$k_s = (1 - z_1)k_1, k_p = (z_2^{-1} - 1)k_2 \quad (27)$$

for s- and p-peaks, respectively. The possibility to substitute k in $G_{s,p}^i$ is justified by the fact that the difference $G_s^i(k, \ldots) - G_s^i(k_s, \ldots)$ is exactly zero in the peak, and therefore, respective integration of this difference divided by kk_1 does not result in the leading log RC.

The integration of (26) over angular variables can be formally presented as

$$\frac{d^3k}{k_0}\frac{1}{k_1 k} = 2\pi l_m dz_1, \qquad \frac{d^3k}{k_0}\frac{1}{k_2 k} = 2\pi l_m \frac{dz_2}{z_2^2}, \quad (28)$$

where

$$l_m = \log\frac{Q^2}{m^2}. \quad (29)$$

The above procedure can be formalized in terms of leptonic tensor (19), which splits in two respective parts in the leading log approximation:

$$L_{Rs}^{\mu\nu} = \frac{1+z_1^2}{z_1(1-z_1)} \frac{1}{k_1 k} L_B^{\mu\nu}(k_1 \to z_1 k_1),$$

$$L_{Rp}^{\mu\nu} = \frac{1+z_2^2}{1-z_2} \frac{1}{k_2 k} L_B^{\mu\nu}(k_2 \to k_2/z_2). \tag{30}$$

The convolution with the hadronic tensor is

$$\begin{aligned} L_R^{\mu\nu} W_{\mu\nu}(q-k, p, p_h) &= L_{Rs}^{\mu\nu} W_{\mu\nu}(q-k_s, p, p_h) \\ &+ L_{Rp}^{\mu\nu} W_{\mu\nu}(q-k_p, p, p_h). \end{aligned} \tag{31}$$

This approach has a useful geometric interpretation. We see that the matrix element squared is calculated as the convolution of the Born leptonic tensor with a shifted momentum of an initial (or final) electron for s- (and p-) peaks. This means the parametrization (27) allows one o write collinear bremsstrahlung in terms of the Born cross section but in a so-called shifted born condition

$$\begin{aligned} z_1 k_1 + p &= k_2 + p_h + p_x, \\ k_1 + p &= k_2/z_2 + p_h + p_x. \end{aligned} \tag{32}$$

The kinematics of the process is sketched in Fig. 3. The momentum transfer $q = k_1 - k_2$ is chosen along the axis z, and vectors k_1, k_2 constitute the x, z-plane. This fixes the coordinate system. In the leading approximation $k \to (1 - z_1)k_1$ or $k \to (1/z_2 - 1)k_2$ lies entirely in the xz-plane.

After substitution of (21), (30), and (27) into (20) and taking into account the angular integration of the first order poles (28), one can find that the leading order approximation of the real photon emission to s- and p-peaks can be
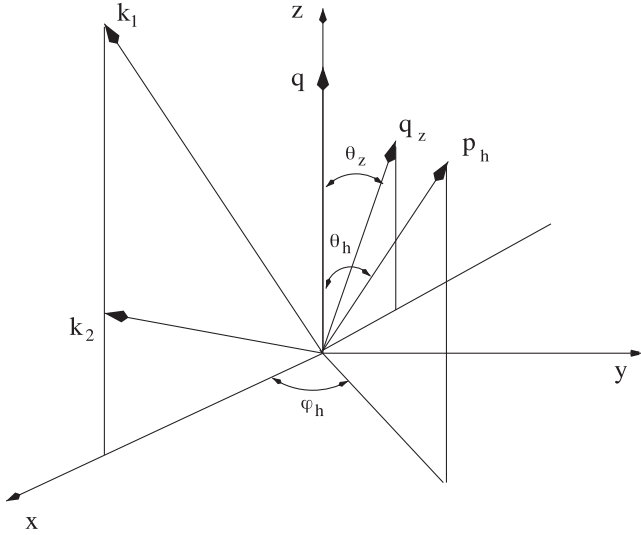

FIG. 3. The momenta of the particles of SIDIS process (2) in the lab frame; q and q_z are the momenta of the virtual photon in the original and shifted kinematics.

expressed through the Born contribution σ_B (13) with so-called shifted variables in the following way:

$$\begin{aligned} d\sigma_{1L}^{\text{ins}} &= \frac{\alpha}{2\pi} l_m dz_1 \frac{1+z_1^2}{1-z_1} \frac{p_{ls}S_x^2}{p_l(z_1 S - X)^2} \\ &\times \sigma_B(z_1 S, z_1 Q^2, x_s, z_s, p_{ts}, \cos\phi_{hs}), \\ d\sigma_{1L}^{\text{inp}} &= \frac{\alpha}{2\pi} l_m dz_2 \frac{1+z_2^2}{z_2^2(1-z_2)} \frac{p_{lp}S_x^2}{p_l(S - X/z_2)^2} \\ &\times \sigma_B(S, z_2^{-1}Q^2, x_p, z_p, p_{tp}, \cos\phi_{hp}). \end{aligned} \tag{33}$$

The quantities with the subscripts s and p read:

$$x_s = \frac{z_1 Q^2}{(z_1 S - X)}, \qquad z_s = \frac{zS_x}{(z_1 S - X)},$$

$$\lambda_{Ys} = (z_1 S - X)^2 + 4z_1 M^2 Q^2,$$

$$p_{ls} = \frac{zS_x(z_1 S - X) - 2M^2(z_1 V_1 - V_2)}{2M\sqrt{\lambda_{Ys}}},$$

$$p_{ts} = \sqrt{\frac{z^2 S_x^2}{4M^2} - p_{ls}^2 - m_h^2},$$

$$\begin{aligned} \cos\phi_{hs} = \frac{1}{4z_1 p_{ts}\sqrt{\lambda_{Ys}\lambda_1}} [&(z_1 S + X)(2z_1 zS_x Q^2 \\ &+ (z_1 S - X)(z_1 V_1 - V_2)) - \lambda_{Ys}(z_1 V_1 + V_2)], \end{aligned}$$

$$x_p = \frac{Q^2}{(z_2 S - X)}, \qquad z_p = \frac{zS_x}{(S - z_2^{-1}X)},$$

$$\lambda_{Yp} = (S - z_2^{-1}X)^2 + 4z_2^{-1}M^2 Q^2,$$

$$p_{lp} = \frac{zS_x(S - z_2^{-1}X) - 2M^2(V_1 - z_2^{-1}V_2)}{2M\sqrt{\lambda_{Yp}}},$$

$$p_{tp} = \sqrt{\frac{z^2 S_x^2}{4M^2} - p_{lp}^2 - m_h^2},$$

$$\begin{aligned} \cos\phi_{hp} = \frac{z_2}{4p_{tp}\sqrt{\lambda_{Yp}\lambda_1}} [&(S + z_2^{-1}X)(2z_2^{-1}zS_x Q^2 \\ &+ (S - z_2^{-1}X)(V_1 - z_2^{-1}V_2)) - \lambda_{Yp}(V_1 + z_2^{-1}V_2)]. \end{aligned} \tag{34}$$

The expressions (33) are infrared divergent at $z_{1,2} \to 1$. This infrared divergence is canceled in the sum with the contribution from the vertex function presented by the Feynman graph in Fig. 1(a).

In the leading log approximation the incorporation of the vertex function contribution and respective cancellation of the infrared divergence is implemented using the electron splitting function, which was originally suggested for use in QCD [9–11] and then was adapted for real photon emission [13,14]. The splitting function is defined through the so-called (+)-operator,

$$P(z) = \frac{1 + z^2}{(1 - z)_+}, \tag{35}$$

and is used to replace the factor $(1 + z^2)/(1 - z)$ in the leading log formulas. This $(+)$-operator is defined as

$$\int_x^1 dz P(z) f(z) = \int_x^1 dz \frac{1 + z^2}{1 - z} (f(z) - f(1))$$
$$- f(1) \int_0^x dz \frac{1 + z^2}{1 - z}. \tag{36}$$

The application of the splitting function to Eq. (33) leads to

$$\sigma_{1L}^{\text{ins}} = \frac{\alpha}{2\pi} l_m \int_{z_{1i}}^1 dz_1 P(z_1) \frac{p_{ls} S_x^2}{p_l (z_1 S - X)^2}$$
$$\times \sigma_B(z_1 S, z_1 Q^2, x_s, z_s, p_{ts}, \cos \phi_{hs}),$$

$$\sigma_{1L}^{\text{inp}} = \frac{\alpha}{2\pi} l_m \int_{z_{2i}}^1 \frac{dz_2}{z_2^2} P(z_2) \frac{p_{lp} S_x^2}{p_l (S - X/z_2)^2}$$
$$\times \sigma_B(S, z_2^{-1} Q^2, x_p, z_p, p_{tp}, \cos \phi_{hp}). \tag{37}$$

The lowest limits of integration can be found through the SIDIS pion threshold

$$z_{1i} = 1 - (p_x^2 - M_{\text{th}}^2)/S',$$
$$z_{2i} = \frac{1}{(1 + (p_x^2 - M_{\text{th}}^2)/X')}. \tag{38}$$

Here M_{th} is the minimal value of the invariant mass of the undetected hadrons p_x for the SIDIS process, e.g., $M_{\text{th}} = M + m_\pi$ when the detected hadron is the pion.

The final expression for the RC in SIDIS in the leading log approximation is

$$\sigma_{1L}^{\text{in}} = \left[1 + \frac{\alpha}{\pi} \delta_{\text{vac}}^l(Q^2) \right] \sigma_B(S, Q^2, x, z, p_t, \phi_h) + \sigma_{1L}^{\text{ins}} + \sigma_{1L}^{\text{inp}}$$

$$= \left[1 + \frac{\alpha}{\pi} \delta_{\text{vac}}^l(Q^2) \right] \sigma_B(S, Q^2, x, z, p_t, \phi_h)$$

$$+ \frac{\alpha}{2\pi} l_m \int_0^1 dz_1 \frac{1 + z_1^2}{1 - z_1} \left[\theta(z_1 - z_{1i}) \frac{p_{ls} S_x^2}{p_l S_{xs}^2} \sigma_B(z_1 S, z_1 Q^2, x_s, z_s, p_{ts}, \cos \phi_{hs}) - \sigma_B(S, Q^2, x, z, p_t, \cos \phi_h) \right]$$

$$+ \frac{\alpha}{2\pi} l_m \int_0^1 dz_2 \frac{1 + z_2^2}{1 - z_2} \left[\frac{\theta(z_2 - z_{2i})}{z_2^2} \frac{p_{lp} S_x^2}{p_l S_{xp}^2} \sigma_B(S, z_2^{-1} Q^2, x_p, z_p, p_{tp}, \cos \phi_{hp}) - \sigma_B(S, Q^2, x, z, p_t, \cos \phi_h) \right]. \tag{39}$$

Here we added the contribution of vacuum polarization by electron [Fig. 1(b)] in leading approximation which is external to the approach involving the splitting function and has to be added separately:

$$\delta_{\text{vac}}^l(Q^2) = \frac{2}{3} l_m. \tag{40}$$

A direct proof that the splitting function works for SIDIS is presented in Appendix (A).

A similar calculation can be applied for extracting the leading approximation from the exclusive radiative tail depicted in Figs. 1(e) and 1(g):

$$l(k_1) + n(p) \to l(k_2) + h(p_h) + u(p_u) + \gamma(k), \tag{41}$$

where p_u is the four-momentum of a single undetected hadron ($p_u^2 = m_u^2$). This process gives the contribution to SIDIS because the mass square of the undetected particles $(p_u + k)^2$ can exceed the pion threshold M_{th}^2 for the rather hard photon emission. As a result the exclusive radiative tail does not contain infrared divergence. Moreover, since the fifth SIDIS variable z is fixed by the energy of the emitted photon in leading approximation photonic variables $z_{1,2}$ are also fixed. The explicit expression for the exclusive radiative tail in the leading approximation is presented below by Eq. (88) of Sec. IV.

B. Extraction leading log correction from exact equations

The expression for the lowest order RC calculated exactly in [8] is

$$\sigma^{in} = \left[1 + \frac{\alpha}{\pi}(\delta_{VR} + \delta^l_{vac} + \delta^h_{vac})\right]\sigma^B(S, Q^2, x, z, p_t, \phi_h)$$
$$+ \sigma^F_R + \sigma^{AMM}. \qquad (42)$$

Two quantities, δ^h_{vac} (σ^{AMM}), do not contribute to RC in the leading approximation, since δ^h_{vac} is independent of the electron mass and σ^{AMM} is proportional to it. The expressions for δ_{VR} and δ^l_{vac} in the leading approximation are presented in Eqs. (A7) and (40), respectively.

The exact expression for σ^F_R is defined by Eq. (43) of [8] through the integration over three photonic variables

$$R = 2kp, \qquad \tau = kq/kp, \qquad \phi_k, \qquad (43)$$

where ϕ_k is an angle between $(\mathbf{k}_1, \mathbf{k}_2)$ and $(\mathbf{k}, \mathbf{q})$ planes

$$\sigma^F_R = -\frac{\alpha^3 S S_x^2}{32\pi M p_l \lambda_S \sqrt{\lambda_Y}} \int_{\tau_{min}}^{\tau_{max}} d\tau \int_0^{2\pi} d\phi_k \int_0^{R_{max}} dR$$

$$\times \sum_{i=1}^4 \left[\sum_{j=1}^3 \frac{\mathcal{H}_i(Q^2 + \tau R, \tilde{x}, \tilde{z}, \tilde{p}_t)\theta^0_{ij}R^{j-2}}{(Q^2 + \tau R)^2}\right.$$

$$\left. - \frac{\theta^0_{i1}\mathcal{H}_i(Q^2, x, z, p_t)}{RQ^4}\right]. \qquad (44)$$

Here the variables with tildes are defined as

$$\tilde{x} = \frac{Q^2 + \tau R}{S_x - R}, \qquad \tilde{z} = \frac{z S_x}{S_x - R},$$

$$\tilde{p}_t^2 = \frac{z^2 S_x^2}{4M^2} - \frac{(z S_x(S_x - R) - 2M^2(2V_- - \mu R))^2}{4M^2((S_x - R)^2 + 4M^2(Q^2 + \tau R))} - m_h^2, \quad (45)$$

and have meaning of the usual SIDIS variables in the shifted kinematics. The limits of integrations are

$$R_{max} = \frac{p_x^2 - M_{th}^2}{1 + \tau - \mu}, \qquad \tau_{max/min} = \frac{S_x \pm \sqrt{\lambda_Y}}{2M^2}, \quad (46)$$

where

$$\mu = \frac{kp_h}{kp} = \frac{p_{h0}}{M} + \frac{p_l(2\tau M^2 - S_x)}{M\sqrt{\lambda_Y}}$$

$$- 2M p_t \cos(\phi_h + \phi_k)\sqrt{\frac{(\tau_{max} - \tau)(\tau - \tau_{min})}{\lambda_Y}}. \quad (47)$$

After replacing variable R by

$$R' = (1 + \tau - \mu)R, \qquad (48)$$

the region of integration transforms into cuboid

$$\int_0^{R_{max}} dR \rightarrow \int_0^{p_x^2 - M_{th}^2} \frac{dR'}{1 + \tau - \mu} \qquad (49)$$

that allows us to perform the integration over R' as external.

The quantities θ^0_{ij} ($i = 1, ..., 4$ and $j = 1, ..., 3$) in (44) are defined in Appendix B of [8]. They result from convolution of the leptonic tensor (19) with hadronic structures $w^i_{\mu\nu}$. These quantities contain the terms corresponding to s- and p-peaks, which are localized in (B.5) of [8] and can be presented in our notation as

$$F_d = \frac{R^2}{4kk_1kk_2} = \frac{1}{\tau}\left(\frac{R}{2kk_2} - \frac{R}{2kk_1}\right),$$

$$F_{1+} = \frac{R}{2kk_2} + \frac{R}{2kk_1},$$

$$F_{2\pm} = \frac{R^2}{4kk_2^2} \pm \frac{R^2}{4kk_1^2}, \qquad (50)$$

with

$$\frac{2k_ik}{R} = a_i + b\cos\phi_k, \qquad (51)$$

where

$$a_1 = \frac{Q^2 S_p + \tau(SS_x + 2M^2 Q^2)}{\lambda_Y},$$

$$a_2 = \frac{Q^2 S_p + \tau(XS_x - 2M^2 Q^2)}{\lambda_Y},$$

$$b = -\frac{2M\sqrt{(\tau_{max} - \tau)(\tau - \tau_{min})\lambda_1}}{\lambda_Y}. \qquad (52)$$

The integration of these terms over ϕ_k give ($n = 1, 2$)

$$\int_0^{2\pi} \frac{d\phi_k}{a_n + b\cos\phi_k} = \frac{2\pi}{\sqrt{C_n}},$$

$$\int_0^{2\pi} \frac{d\phi_k}{(a_n + b\cos\phi_k)^2} = \frac{2\pi a_n}{C_n^{3/2}}, \qquad (53)$$

with

$$C_1 = \frac{S^2(\tau - \tau_s)^2 + 4m^2 M^2 (\tau - \tau_{\min})(\tau_{\max} - \tau)}{\lambda_Y},$$

$$C_2 = \frac{X^2(\tau - \tau_p)^2 + 4m^2 M^2 (\tau - \tau_{\min})(\tau_{\max} - \tau)}{\lambda_Y}. \qquad (54)$$

Because of the smallness of the lepton mass the expressions for $C_{1,2}$ have a sharp peak for $\tau \to \tau_s \equiv -Q^2/S$ and $\tau \to \tau_p \equiv Q^2/X$, respectively. Note the quantities $\tau_{s,p}$ can also be obtained from $\tau = kq/kp$ by the replacement $k \to k_{s,p}$ from (27).

The integration over τ of expressions (53) can be performed analytically,

$$\int\limits_{\tau_{\min}}^{\tau_{\max}} d\tau \int\limits_0^{2\pi} \frac{d\phi_k}{a_1 + b\cos\phi_k} = 2\pi\sqrt{\lambda_Y} L_S,$$

$$\int\limits_{\tau_{\min}}^{\tau_{\max}} d\tau \int\limits_0^{2\pi} \frac{d\phi_k}{a_2 + b\cos\phi_k} = 2\pi\sqrt{\lambda_Y} L_X,$$

$$\int\limits_{\tau_{\min}}^{\tau_{\max}} d\tau \int\limits_0^{2\pi} \frac{d\phi_k}{(a_i + b\cos\phi_k)^2} = \frac{2\pi\sqrt{\lambda_Y}}{m^2}, \qquad (55)$$

with

$$L_S = \frac{1}{\sqrt{\lambda_S}} \log \frac{S + \sqrt{\lambda_S}}{S - \sqrt{\lambda_S}}$$
$$= \frac{1}{S}\left[l_m + \log\frac{S^2}{Q^2 M^2} \right] + \mathcal{O}\left(\frac{m^2}{Q^2}\right),$$

$$L_X = \frac{1}{\sqrt{\lambda_X}} \log \frac{X + \sqrt{\lambda_X}}{X - \sqrt{\lambda_X}}$$
$$= \frac{1}{X}\left[l_m + \log\frac{X^2}{Q^2 M^2} \right] + \mathcal{O}\left(\frac{m^2}{Q^2}\right). \qquad (56)$$

We see that only the first order poles ($1/k_1 k$ and $1/k_2 k$) contribute to RC in the leading approximation.

Actually, the integrand in (55) depends on τ and ϕ_k not only in θ_{ij}^0 but also in arguments of structure functions $\mathcal{H}_i$, the photonic propagator squared $(Q^2 + \tau R)^{-2}$, and the factor $(1 + \tau - \mu)$ that appeared after the substitution of the integration variable $R \to R'$ in Eq. (49). All these functions are regular (i.e., equivalent to neither zero nor infinity in the integration region). Therefore, we can make the identical transformation for extraction of the leading and next-to-leading terms:

$$\int\limits_{\tau_{\min}}^{\tau_{\max}} d\tau \int\limits_0^{2\pi} d\phi_k \frac{\mathcal{G}(\tau, \phi_k)}{a_1 + b\cos\phi_k} = 2\pi\sqrt{\lambda_Y} L_S \mathcal{G}(\tau_s, 0) + \int\limits_{\tau_{\min}}^{\tau_{\max}} d\tau \int\limits_0^{2\pi} d\phi_k \frac{\mathcal{G}(\tau, \phi_k) - \mathcal{G}(\tau_s, 0)}{a_1 + b\cos\phi_k},$$

$$\int\limits_{\tau_{\min}}^{\tau_{\max}} d\tau \int\limits_0^{2\pi} d\phi_k \frac{\mathcal{G}(\tau, \phi_k)}{a_2 + b\cos\phi_k} = 2\pi\sqrt{\lambda_Y} L_X \mathcal{G}(\tau_p, 0) + \int\limits_{\tau_{\min}}^{\tau_{\max}} d\tau \int\limits_0^{2\pi} d\phi_k \frac{\mathcal{G}(\tau, \phi_k) - \mathcal{G}(R', \tau_p, 0)}{a_2 + b\cos\phi_k}, \qquad (57)$$

where $\mathcal{G}(\tau, \phi_k)$ is a regular function of τ and ϕ_k. The second terms in the right-hand side of these transformations do not include the leading terms and vanish in our approximation.

Following Eq. (57) the quantities θ_{ij}^0 from (44) can be decomposed as

$$\theta_{ij}^0 = \frac{\theta_{ij}^s}{a_1 + b\cos\phi_k} + \frac{\theta_{ij}^p}{a_2 + b\cos\phi_k} + \theta_{ij}^{\text{rest}}, \qquad (58)$$

where the quantities θ_{ij}^s and θ_{ij}^p contain the terms proportional to $1/kk_1$ and $1/kk_2$ and are independent of the integration variables τ and ϕ_k. They are obtained in the limit $m \to 0$, $\phi_k = 0$, and $\tau \to \tau_s$ and $\tau \to \tau_p$ for s- and p-peaks, respectively. The quantity μ at the peaks become $\mu \to \mu_s \equiv V_1/S$ and $\mu \to \mu_p \equiv V_1/X$. The last term in Eq. (58), $\theta_{ij}^{\text{rest}}$, does not give the contribution to the leading approximation.

The quantities θ_{ij}^s and θ_{ij}^p are expressed in terms of respective Born θ_i^B defined in Eq. (14)

$$\theta_{ij}^{s,p} = d_j^{s,p} \theta_i^B, \qquad (59)$$

where

$$d_1^s = -4S, \qquad d_2^s = 4, d_3^s = -\frac{2}{S},$$

$$d_1^p = -4X, \qquad d_2^p = 4, d_3^p = -\frac{2}{X}. \qquad (60)$$

Then the sums over j can be explicitly calculated:

$$\sum_{j=1}^{3}\left[\frac{R'}{1+\tau_s-\mu_s}\right]^{j-2}d_j^s = -2\frac{(S'-R')^2+S'^2}{S'R'},$$

$$\frac{(1+\tau_s-\mu_s)}{R'}d_1^s = -4\frac{S'}{R'},$$

$$\sum_{j=1}^{3}\left[\frac{R'}{1+\tau_p-\mu_p}\right]^{j-2}d_j^p = -2\frac{(X'+R')^2+X'^2}{X'R'},$$

$$\frac{(1+\tau_p-\mu_p)}{R'}d_1^p = -4\frac{X'}{R'}, \qquad (61)$$

where we used $1+\tau_s-\mu_s = S'/S$ and $1+\tau_p-\mu_p = X'/X$.

Substitution of the decomposition (58) into (44) results in the separation of σ_R^F into two parts corresponding to s- and p-collinear singularities. Integration over R' can be further replaced by z_1 and z_2 for these two parts using the substitutions $R' \to (1-z_1)S'$ and $R' \to (z_2^{-1}-1)X'$:

$$\int_0^{p_x^2-M_{th}^2} dR' \to S'\int_{z_{1i}}^1 dz_1,$$

$$\int_0^{p_x^2-M_{th}^2} dR' \to X'\int_{z_{2i}}^1 \frac{dz_2}{z_2^2}, \qquad (62)$$

where the lowest limits of integration over variables $z_{1,2}$ are defined by Eq. (38). The expressions from the right-hand side (rhs) of Eq. (61) are reduced as

$$\frac{(S'-R')^2+S'^2}{S'R'} = \frac{1+z_1^2}{1-z_1},$$

$$\frac{(X'+R')^2+X'^2}{X'R'} = \frac{1+z_2^2}{z_2(1-z_2)}. \qquad (63)$$

The obtained equations are combined as follows resulting in final expressions in the leading log approximation. The substitution of Eq. (58) into (44) with dropped θ_{ij}^{rest} splits the expression σ_R^F into two parts that correspond to s- and p-peaks according to the upper index in the first and second terms of θ_{ij} in the rhs of Eq. (58): $\sigma_R^F = \sigma_s^F + \sigma_s^F$. Integration over τ and ϕ_k is performed using (57) in which the second terms in the rhs have to be dropped. The arguments of the structure functions $\mathcal{H}_i(Q^2+\tau R, \tilde{x}, \tilde{z}, \tilde{p}_t)$ are transferred into $\mathcal{H}_i(z_1Q^2, x_s, z_s, p_{ts})$ or $\mathcal{H}_i(z_2^{-1}Q^2, x_p, z_p, p_{tp})$ for s- or p-peaks, respectively, where the quantities with the subscripts s and p are defined by Eq. (38). Finally, the representation of $\theta_{ij}^{s,p}$ in the form of (59) and (60) allows us to perform summation over j as it was shown in Eq. (61) and to obtain the final expressions in the form

$$\sigma_s^F = \frac{\alpha^3 S_x^2}{8Mp_lS}l_m\int_{z_{1i}}^1 dz_1\sum_{i=1}^4\left[\frac{1+z_1^2}{1-z_1}\frac{\mathcal{H}_i(z_1Q^2,x_s,z_s,p_{ts})\theta_i^B}{z_1^2Q^4} - 2\frac{\theta_i^B\mathcal{H}_i(Q^2,x,z,p_t)}{(1-z_1)Q^4}\right],$$

$$\sigma_p^F = \frac{\alpha^3 S_x^2}{8Mp_lS}l_m\int_{z_{2i}}^1 \frac{dz_2}{z_2^2}\sum_{i=1}^4\left[\frac{1+z_2^2}{z_2(1-z_2)}\frac{z_2^2\mathcal{H}_i(z_2^{-1}Q^2,x_p,z_p,p_{tp})\theta_i^B}{Q^4} - 2\frac{\theta_i^B\mathcal{H}_i(Q^2,x,z,p_t)}{(1-z_2)Q^4}\right]. \qquad (64)$$

Using Eq. (13) we represent the products of θ_i^B and $\mathcal{H}_i$ through the Born cross section in the shifted kinematics for s- and p-peaks, respectively,

$$\frac{\mathcal{H}_i(z_1Q^2,x_s,z_s,p_{ts})\theta_i^B}{z_1^2Q^4}$$

$$= \frac{4M^2p_{ls}S}{\pi\alpha^2(z_1S-X)^2}\sigma_B(z_1S,z_1Q^2,x_s,z_s,p_{ts},\cos\phi_{hs}),$$

$$\frac{z_2^2\mathcal{H}_i(z_2^{-2}Q^2,x_p,z_p,p_{tp})\theta_i^B}{Q^4}$$

$$= \frac{4M^2p_{lp}S}{\pi\alpha^2(S-z_2^{-1}X)^2}\sigma_B(S,z_2^{-1}Q^2,x_p,z_p,p_{tp},\cos\phi_{hp}), \qquad (65)$$

and obtain the expressions (A3) and, after cancellation of the infrared divergence, (A6). Finally, the expressions in the leading log approximation (39) can be obtained from (A6) using the integral representation for δ_{VR} that is defined by Eq. (A7). Indeed, the difference between (A3) and (39) is exactly $\alpha/\pi\delta_{VR}\sigma^B$:

$$\delta_{VR} = \frac{l_m}{2}\left[\int_{z_{1i}}^1 dz_1(1+z_1) - \int_0^{z_{1i}} dz_1\frac{1+z_1^2}{1-z_1}\right.$$

$$\left. + \int_{z_{2i}}^1 dz_2\frac{2+z_2+z_2^2}{z_2} - \int_0^{z_{2i}} dz_2\frac{1+z_1^2}{1-z_1}\right]. \qquad (66)$$
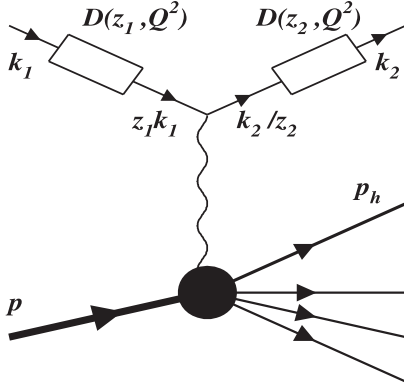
FIG. 4. The cross section in the methods of the electron structure functions.

C. Electron structure function method

Up to now the lowest order RC to SIDIS in the leading approximation have been considered. The second order RC to the cross section of unpolarized inclusive DIS within leading order were first estimated by Kripfganz, Mohring, and Spiesberger in [14] and were generalized to polarized DIS by our group [28]. The approach to summing up the leading logarithmic RC of all orders over α that involves the electron structure function was suggested by Fadin, Merenkov, and Kuraev in [20,21]. This method was applied for polarized inclusive DIS in [22]. The main features of the method of the electron structure functions as well as the detailed comparison between different approaches for the calculation of RC to polarized inclusive DIS are presented in [23].

The cross section of SIDIS within the method of electron structure functions (illustrated in Fig. 4) reads

$$
\sigma_{hL}^{in} = \frac{S_x^2}{p_l} \int\limits_{z_{1i}}^{1} dz_1 D(z_1, Q^2) \int\limits_{\hat{z}_{2i}}^{1} \frac{dz_2}{z_2^2} D(z_2, Q^2)
$$
$$
\times r^2 \left(\frac{z_1}{z_2} Q^2 \right) \frac{\hat{p}_l \sigma_{hard}(z_1 S, z_1 z_2^{-1} Q^2, \hat{x}, \hat{z}, \hat{p}_t, \cos\hat{\phi}_h)}{(z_1 S - X/z_2)^2},
$$
$$
\tag{67}
$$

where z_{1i} is defined by Eq. (38) and

$$
\hat{z}_{2i} = \left[1 + \frac{p_x^2 - (1 - z_1)S' - M_{th}^2}{X - V_2 + z_1 Q^2} \right]^{-1}. \tag{68}
$$

The electron structure function $D(z_{1,2}, Q^2)$ contains three terms

$$
D = D^\gamma + D_N^{e^+e^-} + D_S^{e^+e^-}, \tag{69}
$$

where D^γ describes the contribution of photon radiation, and $D_N^{e^+e^-}$ and $D_S^{e^+e^-}$ correspond to the process of the

electron pair production in nonsinglet (by the single photon mechanism) and singlet (by the double photon mechanism) channels, respectively [20–23]. The explicit expressions for the components of electron structure function $D(z_{1,2}, Q^2)$ are presented in Eqs. (5)–(7) of [22]. The coefficient r^2 in the integrand in Eq. (67) results from resummation of the vacuum polarization by leptons (40),

$$
r(Q^2) = \sum_{i=0}^{\infty} \left(\frac{\alpha}{2\pi} \delta_{vac}^l(Q^2) \right)^i = \left[1 - \frac{\alpha}{2\pi} \delta_{vac}^l(Q^2) \right]^{-1}, \tag{70}
$$

and represented in the form of the running coupling constant.

The hard cross section, σ_{hard}, in (67) is the radiative corrected SIDIS cross section excluding the leading log term [22],

$$
\sigma_{hard} = \sigma_B + \sigma^{in} - \sigma_{1L}^{in}. \tag{71}
$$

Here σ^{in} and σ_{1L}^{in} are defined by Eqs. (42) and (39), respectively. This cross section is generalized to all orders of α as

$$
\sigma_{hard} = \sigma_B + \sum_{i=1}^{\infty} \alpha^i \sum_{j=0}^{i-1} C_{ij} l_m^j + \mathcal{O}\left(\frac{m^2}{Q^2} \right), \tag{72}
$$

where the coefficients C_{ij} do not depend on the electron mass and are responsible for subleading contributions in each order of α^i. The formula (67) with σ_{hard} given by Eq. (72) is the best approximation of RC from continuous spectrum (i.e., excluding the exclusive radiative tail) in SIDIS processes.

The expressions for the shifted variables in (67) represent the extension of such variables defined by Eq. (40):

$$
\hat{x} = \frac{z_1 Q^2}{z_1 z_2 S - X}, \qquad \hat{z} = \frac{z S_x}{z_1 S - z_2^{-1} X},
$$
$$
\hat{\lambda}_Y = (z_1 S - z_2^{-1} X)^2 + 4 z_1 z_2^{-1} M^2 Q^2,
$$
$$
\hat{p}_l = \frac{z S_x (z_1 S - z_2^{-1} X) - 2M^2 (z_1 V_1 - z_2^{-1} V_2)}{2M \sqrt{\hat{\lambda}_Y}},
$$
$$
\hat{p}_t^2 = \frac{z^2 S_x^2}{4M^2} - \hat{p}_l^2 - m_h^2,
$$
$$
\cos\hat{\phi}_h = \frac{z_2}{4 z_1 \hat{p}_t \sqrt{\hat{\lambda}_Y \lambda_1}} \left[\left(z_1 S + \frac{X}{z_2} \right) \left(2\frac{z_1}{z_2} z S_x \hat{Q}^2 \right. \right.
$$
$$
\left. + \left(z_1 S - \frac{X}{z_2} \right) \left(z_1 V_1 - \frac{V_2}{z_2} \right) \right)
$$
$$
\left. - \hat{\lambda}_Y \left(z_1 V_1 + \frac{V_2}{z_2} \right) \right]. \tag{73}
$$

We note that the expression for the cross section in the leading log approximation in Eq. (39) is reproduced from (67) by keeping the first order (nontrivial) terms in series over α of the electron structure function [29], $r(Q^2)$, and σ_{hard}:

$$
\begin{aligned}
D(z, Q^2) &\to \delta(1 - z) + \frac{\alpha}{2\pi} l_m P(z), \\
r(Q^2) &\to 1 + \frac{\alpha}{\pi} \delta_{\text{vac}}^l(Q^2), \\
\sigma_{\text{hard}} &\to \sigma_B.
\end{aligned}
\tag{74}
$$

IV. APPLYING LEADING LOG RESULT TO EXCLUSIVE RADIATIVE TAIL

The exact contribution calculated in [8] reads

$$
\sigma_R^{ex} = -\frac{\alpha^3 S S_x^2}{2^8 \pi^4 M p_l \lambda_S \sqrt{\lambda_Y}} \int\limits_{\tau_{\min}}^{\tau_{\max}} d\tau \int\limits_0^{2\pi} d\phi_k
$$

$$
\times \sum_{i=1}^4 \sum_{j=1}^3 \frac{\mathcal{H}_i^{ex}(Q^2 + \tau R_{ex}, \tilde{W}_{ex}^2, \tilde{t}_{ex}) \theta_{ij}^0 R_{ex}^{j-2}}{(1 + \tau - \mu)(Q^2 + \tau R_{ex})^2},
\tag{75}
$$

where

$$
R_{ex} = \frac{p_x^2 - m_u^2}{1 + \tau - \mu}, \qquad \tilde{W}_{ex}^2 = W^2 - (1 + \tau R_{ex}),
$$

$$
\tilde{t}_{ex} = t + R_{ex}(\mu - \tau).
\tag{76}
$$

The leading log terms can be extracted from θ_{ij}^0 using methods of Sec. III B. For these analyses it is necessary to keep in mind that only angular integrations, i.e., over τ and ϕ_k, have to be performed for the exclusive tail. However, in the present section we will use results of Eqs. (37) and (67).

Similar to SIDIS the Born cross section of the exclusive process,

$$
l(k_1) + n(p) \to l(k_2) + h(p_h) + u(p_u)
\tag{77}
$$

$(p_u^2 = m_u^2)$, can be presented in the form of convolution leptonic and hadronic tensors (9)

$$
d\sigma_B^{ex} = \frac{(4\pi\alpha)^2}{2SQ^4} W_{\mu\nu}^{ex}(q, p, p_h) L_B^{\mu\nu} d\Gamma_B^{ex}.
\tag{78}
$$

$L_B^{\mu\nu}$ was defined earlier by Eq. (11), whereas

$$
W_{\mu\nu}^{ex}(q, p, p_h) = \sum_{i=1}^4 w_{\mu\nu}^i(q, p, p_h) \mathcal{H}_i^{ex}
\tag{79}
$$

and the quantities $w_{\mu\nu}^i$ have the same structure as in (12). As it was presented in Appendix A of [7], the exclusive structure functions $\mathcal{H}_i^{ex}$ can be expressed through the

standard set of the twofold cross sections $d\sigma_L/d\Omega$, $d\sigma_T/d\Omega$, $d\sigma_{LT}/d\Omega$, and $d\sigma_{TT}/d\Omega$.

The phase space can be expressed through $d\Gamma_B$ (10) as

$$
d\Gamma_B^{ex} = d\Gamma_B \frac{d^3 p_u}{(2\pi)^3 2p_{u0}} \delta^4(p + k_1 - k_2 - p_h - p_u).
\tag{80}
$$

As a result

$$
\begin{aligned}
\frac{d\sigma_B^{ex}}{dxdydzdp_t^2 d\phi_h} &= \frac{1}{(2\pi)^3} \delta\left(\frac{\sqrt{\lambda_Y} p_l}{M} + W^2 + m_h^2 - m_u^2 \right. \\
&\left. - \frac{zS_x(S_x + 2M^2)}{2M^2}\right) \frac{\pi\alpha^2 S_x^2}{4MQ^4 p_l S} \sum_{i=1}^4 \theta_i^B \mathcal{H}_i^{ex} \\
&= \delta(z_0 - z) \bar{\sigma}_B^{ex}(S, Q^2, x, p_t^2, \cos\phi_h),
\end{aligned}
\tag{81}
$$

where

$$
z_0 = \frac{2M(\sqrt{\lambda_Y} p_l + M(W^2 + m_h^2 - m_u^2))}{S_x(S_x + 2M^2)}.
\tag{82}
$$

Here and below the symbol $\bar{\sigma}^{ex}$ is used to denote the fourfold cross section of exclusive processes, and the original symbol σ^{ex} is kept to represent the fivefold contribution of exclusive processes to RC to the SIDIS cross section.

After tensor convolution and integration over z using the δ-function, the Born cross section of the exclusive process reads

$$
\begin{aligned}
\bar{\sigma}_B^{ex}(S, Q^2, x, p_t, \cos\phi_h) &\equiv \frac{d\sigma_B^{ex}}{dxdydp_t^2 d\phi_h} \\
&= \frac{\alpha^2 M S_x}{16\pi^2 Q^4 S p_l (S_x + 2M^2)} \\
&\times \sum_{i=1}^4 \mathcal{H}_i^{ex}(Q^2, W^2, t) \theta_i^B.
\end{aligned}
\tag{83}
$$

Here for the exclusive process

$$
\begin{aligned}
p_t^2 &= p_{h0}^2 - p_l^2 - m_h^2, \\
p_l &= \frac{S_x(W^2 + m_h^2 - m_u^2) - 2V_-(S_x + 2M^2)}{2M\sqrt{\lambda_Y}}, \\
p_{h0} &= \frac{W^2 + m_h^2 - m_u^2 - 2V_-}{2M}.
\end{aligned}
\tag{84}
$$

The general leading log formulas are given by expressions (37). These formulas are applicable for the contribution of the exclusive radiative tail to the SIDIS process in which the fivefold cross section (81) has to be used for σ_B in (37). However, the cross section (81) contains the δ-function because of the fixed mass of the unobserved hadronic state. This δ-function is used to integrate over z_1

or z_2, so the final expressions do not contain the integration as in (39) and expressed in terms of the fourfold born cross section of exclusive process (83). We demonstrate the derivation of the leading log formulas for the exclusive radiative tail by obtaining the formulas for the cross section (81) in s- and p-peaks (i.e., in the shifted kinematics) and analytic integration using the δ-function.

The phase space in the shifted kinematics for s- and p-peaks is

$$
\begin{aligned}
d\Gamma_B^{\text{exs}} &= d\Gamma_B^s \frac{d^3 p_u}{(2\pi)^3 2 p_{u0}} \delta^4(p + z_1 k_1 - k_2 - p_h - p_u) \\
&= \frac{1}{(2\pi)^3} d\Gamma_B^s \delta(M^2 + m_h^2 - m_u^2 - z S_x + z_1 S' + V_2 - X), \\
d\Gamma_B^{\text{exp}} &= d\Gamma_B^p \frac{d^3 p_u}{(2\pi)^3 2 p_{u0}} \delta^4(p + k_1 - k_2/z_2 - p_h - p_u) \\
&= \frac{1}{(2\pi)^3} d\Gamma_B^s \delta(M^2 + m_h^2 - m_u^2 - z S_x + S - V_1 - X/z_2),
\end{aligned} \tag{85}
$$

where $d\Gamma_B^{s,p}$ are the phase spaces for SIDIS Born processes in the shifted kinematics.

As a result

$$
\begin{aligned}
\frac{d\sigma_B^{\text{exs}}}{dx_s dy_s dz_s dp_{ts}^2 d\phi_{hs}} &= \frac{1}{(2\pi)^3} \delta(M^2 + m_h^2 - m_u^2 - z S_x + z_1 S' + V_2 - X) \frac{\pi\alpha^2 (z_1 S - X)^2}{4 z_1^3 M Q^4 p_{ls} S} \sum_{i=1}^4 \theta_{is}^B \mathcal{H}_{is}^{ex}, \\
\frac{d\sigma_B^{\text{exp}}}{dx_p dy_p dz_p dp_{tp}^2 d\phi_{hp}} &= \frac{1}{(2\pi)^3} \delta(M^2 + m_h^2 - m_u^2 - z S_x + S - V_1 - X/z_2) \frac{\pi\alpha^2 z_2 (S - X/z_2)^2}{4 M Q^4 p_{lx} S} \sum_{i=1}^4 \theta_{ip}^B \mathcal{H}_{ip}^{ex}.
\end{aligned} \tag{86}
$$

After the substitution of (86) into Eq. (37) taking into account that for the exclusive process M_{th}^2 incoming into (38) is equal to the undetected hadron mass square m_u^2 after integration over $z_{1,2}$, we can obtain that

$$
\sigma_{1L}^{ex} = \sigma_{1L}^{\text{exs}} + \sigma_{1L}^{\text{exp}}, \tag{87}
$$

where

$$
\begin{aligned}
\sigma_{1L}^{\text{exs}} &= \frac{\alpha}{2\pi} l_m \frac{1 + z_{1e}^2}{1 - z_{1e}} \frac{p_{lse}}{p_l} \frac{S_x^2}{S'} \left[\frac{1}{z_{1e} S - X} + \frac{1}{2M^2} \right] \\
&\quad \times \bar{\sigma}_B^{ex}(z_{1e} S, z_{1e} Q^2, x_{se}, p_{tse}, \cos\phi_{hse}), \\
\sigma_{1L}^{\text{exp}} &= \frac{\alpha}{2\pi} l_m \frac{1 + z_{2e}^2}{1 - z_{2e}} \frac{p_{lpe}}{p_l} \frac{S_x^2}{X'} \left[\frac{1}{S - X/z_{2e}} + \frac{1}{2M^2} \right] \\
&\quad \times \bar{\sigma}_B^{ex}(S, Q^2/z_{2e}, x_{pe}, p_{tpe}, \cos\phi_{hpe}),
\end{aligned} \tag{88}
$$

and the quantities $z_{1,2e}$ are defined using Eq. (38) as

$$
z_{1,2e} = z_{1,2i}(M_{\text{th}}^2 \to m_u^2). \tag{89}
$$

The variables with the indexes se (pe) are calculated from Eq. (34) using the following replacements: (i) $z_1 \to z_{1e}$

and $z \to (M^2 + m_h^2 - m_u^2 + z_{1e} S' + V_2 - X)/S_x$ for σ_{1L}^{exs}, and (ii) $z_2 \to z_{2e}$ and $z \to (M^2 + m_h^2 - m_u^2 + X'/z_{2e} + S - V_1)/S_x$ for σ_{1L}^{exp}.

The generalization on the high orders is performed similarly to (67). This formula is applicable to the case of the exclusive radiative tail; however, again, the σ_{hard} in (67) has to be presented through the product of the fourfold cross section and respective δ-function. This δ-function is then used to integrate over one of two integration variables z_1 or z_2:

$$
\begin{aligned}
d\hat{\Gamma}_B^{ex} &= d\hat{\Gamma}_B \frac{d^3 p_u}{(2\pi)^3 2 p_{u0}} \delta^4(p + z_1 k_1 - k_2/z_2 - p_h - p_u) \\
&= \frac{1}{(2\pi)^3} d\hat{\Gamma}_B \delta(M^2 + m_h^2 - m_u^2 - z S_x \\
&\quad - z_1 z_2^{-1} Q^2 + z_1(S - V_1) + z_2^{-1}(V_2 - X)).
\end{aligned} \tag{90}
$$

We can use (67) with $M_{\text{th}}^2 = m_u^2$. As a result,

$$\sigma_{hL}^{ex} = \frac{S_x^2}{p_l} \int\limits_{z_{1e}}^{1} dz_1 D(z_1, Q^2) \int\limits_{\hat{z}_{2e}}^{1} \frac{dz_2}{z_2^2} D(z_2, Q^2)$$

$$\times r^2 \left(\frac{z_1}{z_2} Q^2\right) \hat{p}_l \left[\frac{1}{z_1 S - X/z_2} + \frac{1}{2M^2}\right] \delta(M^2 + m_h^2$$

$$- m_u^2 - z S_x - z_1 z_2^{-1} Q^2 + z_1(S - V_1) + z_2^{-1}(V_2 - X))$$

$$\times \bar{\sigma}_B^{ex}\left(z_1 S, \frac{z_1}{z_2} Q^2, \hat{x}, \hat{p}_t, \cos\hat{\phi}_h\right), \tag{91}$$

FIG. 5. Integration area (blue line) in the plane (z_1, z_2). The quantities $z_{1,2e}$ and z_m are defined by Eqs. (38), (89), and (92).

and the shifted quantities are defined by Eq. (73).

Because of the functional relationship between z_1 and z_2 induced by the δ-function, the integration area in (91) is the solid curve shown in Fig. 5. The integrand has two sharp peaks in the areas when z_1 and z_2 are cclose to 1 which come from the functions $D(z_1, Q^2)$ and $D(z_2, Q^2)$ and are interpreted as s- and p-peaks, respectively. There are two ways to remove the δ-function in (91) performing integration over either z_1 or z_2; however, it is natural to split the integration region by the point C with coordinates (z_m, z_m) (crossing the integration area and the line $z_1 = z_2$; Fig. 5), thus isolating s- and p-peak peaks in separate contributions,
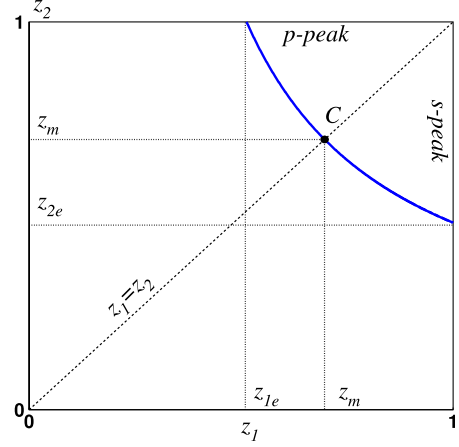
$$z_m = \frac{1}{2(S - V_1)}[S_x + m_u^2 - p_x^2 - 2V_-$$

$$+ \sqrt{(p_x^2 - S_x - m_u^2 + 2V_-)^2 + 4(S - V_1)(X - V_2)}]. \tag{92}$$

The result of this integration is

$$\sigma_{hL}^{ex} = \frac{S_x^2}{p_l} \int\limits_{z_m}^{1} \left[dz_1 \frac{D(z_1, Q^2)D(\hat{z}_2, Q^2)}{X - V_2 + z_1 Q^2} r^2\left(\frac{z_1}{\hat{z}_2} Q^2\right) \hat{p}_{l2} \left[\frac{1}{z_1 S - X/\hat{z}_2} + \frac{1}{2M^2}\right] \right.$$

$$\times \bar{\sigma}_{hard}^{ex}\left(z_1 S, \frac{z_1}{\hat{z}_2} Q^2, \hat{x}_2, \hat{p}_{t2}, \cos\hat{\phi}_{h2}\right) + \frac{dz_2}{z_2^2} \frac{D(\hat{z}_1, Q^2)D(z_2, Q^2)}{S - V_1 - Q^2/z_2} r^2\left(\frac{\hat{z}_1}{z_2} Q^2\right)$$

$$\left. \times \hat{p}_{l1} \left[\frac{1}{\hat{z}_1 S - X/z_2} + \frac{1}{2M^2}\right] \bar{\sigma}_{hard}^{ex}\left(\hat{z}_1 S, \frac{\hat{z}_1}{z_2} Q^2, \hat{x}_1, \hat{p}_{t1}, \cos\hat{\phi}_{h1}\right)\right], \tag{93}$$

where

$$\hat{z}_2 = \left[1 + \frac{p_x^2 - (1 - z_1)S' - m_u^2}{X - V_2 + z_1 Q^2}\right]^{-1},$$

$$\hat{z}_1 = 1 - \frac{p_x^2 + (1 - 1/z_2)X' - m_u^2}{S - V_1 - Q^2/z_2}. \tag{94}$$

The shifted variables in (93) are defined by Eq. (73) with the transformations (i) $z_2 \to \hat{z}_2$ and $z \to (M^2 + m_h^2 - m_u^2 + z_1(S - V_1) + (X - V_2)/\hat{z}_2)/S_x$ for the integrand over z_1 in (93), and (ii) $z_1 \to \hat{z}_1$ and $z \to (M^2 + m_h^2 - m_u^2 + \hat{z}_1 (S - V_1) + (X - V_2)/z_2)/S_x$ for the integrand over z_2.

The cross section $\bar{\sigma}_{hard}^{ex}$ in (93) is the cross section of the exclusive process with the lowest order RC excluding the

leading log terms. The use of this cross section in (93) instead of σ_B^{ex} allows one to account for subleading effects in the RC of higher order. Formally,

$$\bar{\sigma}_{hard}^{ex} = \bar{\sigma}_B^{ex} + \bar{\sigma}_{RC}^{ex} - \bar{\sigma}_{1L}^{ex}, \tag{95}$$

where $\bar{\sigma}_{RC}^{ex}$ is the cross section of exclusive processes with the lowest order RC that is given by Eq. (55) of [30]. We rewrote this cross section in terms of the variables that are used in this analysis, i.e., $d\sigma/(dW^2 dQ^2 d\Omega_h) \to d\sigma/(dxdydp_t^2 d\phi_h)$:

$$\bar{\sigma}_{RC}^{ex} = -\frac{\alpha^3 M S_x}{2^8 \pi^4 (S_x + 2M^2) S Q^2} \int\limits_0^{v_m} dv \int \frac{d\Omega_k}{f}$$

$$\times \sum_{i=1}^4 \left[\frac{\theta_i \mathcal{H}_i^{ex}}{\tilde{Q}^4 (p_l - v/2M\sqrt{\lambda_Y})} - 4F_{IR} \frac{\theta_i^0 \mathcal{H}_i^{ex0}}{\tilde{Q}^4 p_l} \right]$$

$$+ \frac{\alpha}{\pi} (\delta_{VR}^{ex} + \delta_{vac}) \bar{\sigma}_B^{ex}, \tag{96}$$

where

$$\delta_{VR}^{ex} = (l_m - 1) \log \frac{v_m^2}{S'X'} + \frac{3}{2} l_m - 2$$

$$- \frac{1}{2} \log^2 \frac{S'}{X'} + \mathrm{Li}_2\left[1 - \frac{M^2 Q^2}{S'X'}\right] - \frac{\pi^2}{6},$$

$$v_m = W^2 + m_h^2 - m_u^2 - \frac{S_x + 2M^2}{M} m_h. \tag{97}$$

Similarly, the leading order terms are obtained from (58) of [30] and have the form in terms of the variables x, y, p_t^2, and ϕ_h:

$$\bar{\sigma}_{1L}^{ex} = \frac{\alpha}{\pi} \delta_{vac}^l(Q^2) \bar{\sigma}_B^{ex}(S, Q^2, x, p_t, \cos\phi_h)$$

$$+ \frac{\alpha S_x^2}{2\pi p_l S'} l_m \int\limits_{z_{1m}}^1 dz_1 P(z_1) \left[\frac{1}{z_1 S - X} + \frac{1}{2M^2} \right]$$

$$\times p_{ls} \bar{\sigma}_B^{ex}(z_1 S, z_1 Q^2, x_s, p_{ts}, \cos\phi_{hs})$$

$$+ \frac{\alpha S_x^2}{2\pi p_l X'} l_m \int\limits_{z_{2m}}^1 \frac{dz_2}{z_2^2} P(z_2) \left[\frac{1}{S - X/z_2} + \frac{1}{2M^2} \right]$$

$$\times p_{lp} \bar{\sigma}_B^{ex}(S, Q^2/z_2, x_p, p_{tp}, \cos\phi_{hp}), \tag{98}$$

where $\delta_{vac}^l(Q^2)$ is defined by Eq. (40), and the lowest limits of integration has a form

$$z_{1m} = 1 - v_m/S',$$

$$z_{2m} = (1 + v_m/X')^{-1}, \tag{99}$$

and the splitting function $P(z)$ is defined by Eqs. (35) and (36).

V. NUMERICAL RESULTS

The main characteristics used in the RC procedure of experimental data analysis is the RC factor defined as a ratio of the radiative corrected cross section to the Born contribution

$$\delta = \frac{\sigma_{obs}}{\sigma_B}. \tag{100}$$

For numerical estimates we applied the parametrization of the SIDIS structure functions in the Wandzura-Wilczek–type approximation [31]. The exclusive structure functions are expressed through the twofold cross sections $d\sigma_L/d\Omega$, $d\sigma_T/d\Omega$, $d\sigma_{LT}/d\Omega$, and $d\sigma_{TT}/d\Omega$ using MAID2007 parametrization [32]. p_t-dependence of the RC factor, δ, constructed from the Born and observed cross sections of semi-inclusive π^+ electroproduction averaged over ϕ_h is presented in Fig. 6. The solid lines show the total correction, and the dashed lines represent the correction excluding the exclusive radiative tail. The difference between exact and leading RC increases with growing z and p_t. The ϕ_h-dependence of the RC factor constructed from completely differential cross sections are presented in Fig. 7. The RC factor reaches its maximum value at the region near $\phi_h = 180°$ and small z. In certain cases the curves for the RC factor are not smooth, e.g., for angles $\phi_h = 160/200°$ and $\phi_h = 110/260°$ in the right column plots in Fig. 7. This reflects the contributions of the exclusive radiative tail that is not small in these kinematic regions. The RC factor can be both higher and lower than one. The calculated (observed) RC factor is always a trade-off between (i) the exclusive radiative tail contribution that is always positive, (ii) the semi-inclusive RC that can be negative because of the contribution of the vertex function, and (iii) the vacuum polarization contribution that is always positive. The blue lines in Figs. 6 and 7 represent the RC factors calculated using the exact equations (42) and (75). The red and black curves show the RC factor in the leading log approximation in the lowest order (39) and (87) and in all orders with respect to α (67), (93), respectively. In all cases dashed and solid lines show the pure semi-inclusive RC and total RC, where the total RC additionally includes the contribution of the exclusive radiative tails. When estimating the high order effects we restrict our consideration only to the leading orders terms; i.e., in (67) and (93) we put $\sigma_{hard} \equiv \sigma_B$ and $\bar{\sigma}_{hard}^{ex} \equiv \bar{\sigma}_B^{ex}$, respectively. The integrand in Eqs. (67) and (93) contains the cross section of hard photon radiation is the result of numeric multidimensional integration over the kinematics of the photon, so the implementation of Eqs. (67) and (93) to our codes for numeric evaluation of RC would require a new level of results in the software development and will be a subject of a separate analysis.

For purposes of numerical analysis we had to modify the cross sections in (100) to provide a clear and well interpreted comparison of the exact and leading log RC. This is because the difference between the exact and leading log RC comes not only because of the difference in exact and leading log formulas for σ_{in}, which is one of the main focuses of the numerical analysis, but also because of a quite strong effect from the contribution from the vacuum polarization induced by μ- and τ-leptons and hadrons [see Fig. 1(b)] that are not included in the leading log formulas. The latter contribution [denote it as $\delta_{vac}^{nlo}(Q^2)$] is trivial and is not of interest for the numerical comparison, so
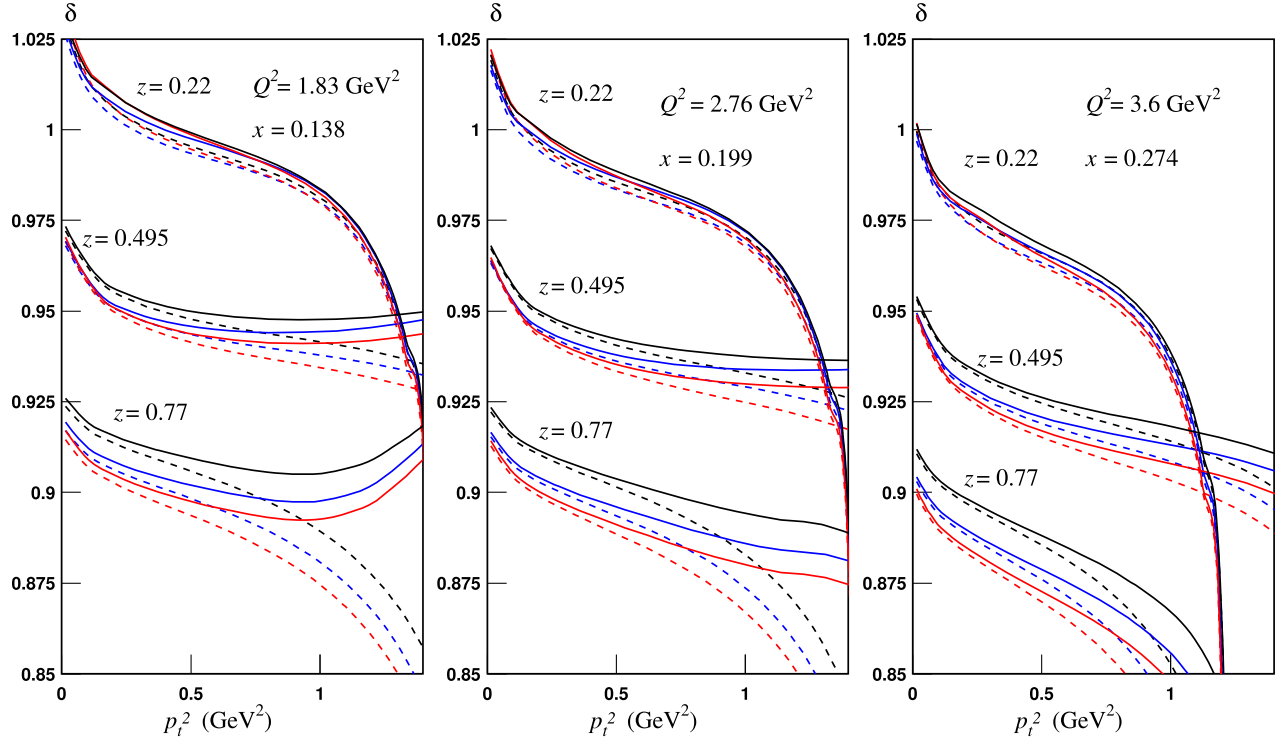
FIG. 6. The p_t-dependence of the RC factor for the cross sections of semi-inclusive π^+ electroproduction averaged over ϕ_h with the lepton beam energy equal to 10.65 GeV. Solid lines show the total RC factor, and dashed lines represent the RC factor calculated excluding the exclusive radiative tail. The blue, red, and black lines show the RC factor calculated exactly, using the methods of the leading log approximation in the lowest order in respect of α and the method of the electron structure functions, respectively.

we added $\delta_{vac}^{nlo}(Q^2)$ to $\delta_{vac}^l(Q^2)$ in Eq. (39) and multiplied the integrand in (67) on $1 + \alpha\delta_{vac}^{nlo}(z_1 Q^2/z_2)/\pi$ to mask its effects on the difference between exact and leading log formulas.

VI. DISCUSSION AND CONCLUSION

In this paper we presented the analytic expressions for RC to the SIDIS cross section derived analytically in the leading log approximation that have a simple analytic form and were not explicitly presented and derived for SIDIS. We demonstrated three distinct approaches allowing for the derivation of the expressions based on different theoretical and computational approaches. The ways in which the results are derived clarify a quite complicated structure of the exact formulas in [8] and further convince theoreticians and experimentalists dealing with practical data analyses in modern SIDIS measurements to use these results in data analyses and Monte Carlo generators.

Specifically, we calculated RC in the leading log approximation using three different approaches. First, we applied the standard approach in the leading log approximation [9–14,27] and calculated the RC from scratch. In this approach the only terms contributing to the cross section in the leading log approximation are extracted and kept, i.e., the poles that correspond to radiation collinear to initial and final electrons (i.e., the

terms that contain $1/kk_1$ and $1/kk_2$ and do not include the electron mass in the numerator). Integration over the photon angles can be performed analytically. Then, all these terms are combined resulting in the factorized form traditional for leading log calculations, i.e., the Born cross section in the so-called shifted kinematics depicted in Fig. 3 for which the three-vector of the virtual photon is shifted in the scattering plane and the angle of this shift is determined by the photon energy (or equivalent variable $z_{1,2}$ for the photon emitted collinear to the initial or final electron line), so there is a remaining one-dimensional integration variable in the final leading log formulas. This calculation resulted in an exact expression for the term A in (1). The infrared divergence is canceled in the usual way so the final formula (39) is infrared-free. The second approach is based on the explicit extraction of the leading log contribution from the exact formulas presented in [8] by collecting all terms contributing to the RC in the leading log approximation after integration over photon angles, and combined them into the final expression exactly coinciding with the expression obtained in the first approach. Third, we used the method of the electron structure functions [20–22]. In this approach the QED radiative corrections to the corresponding cross sections can be written as a convolution of the two electron structure functions corresponding to multiple real photon emission along with the initial and final electron and the
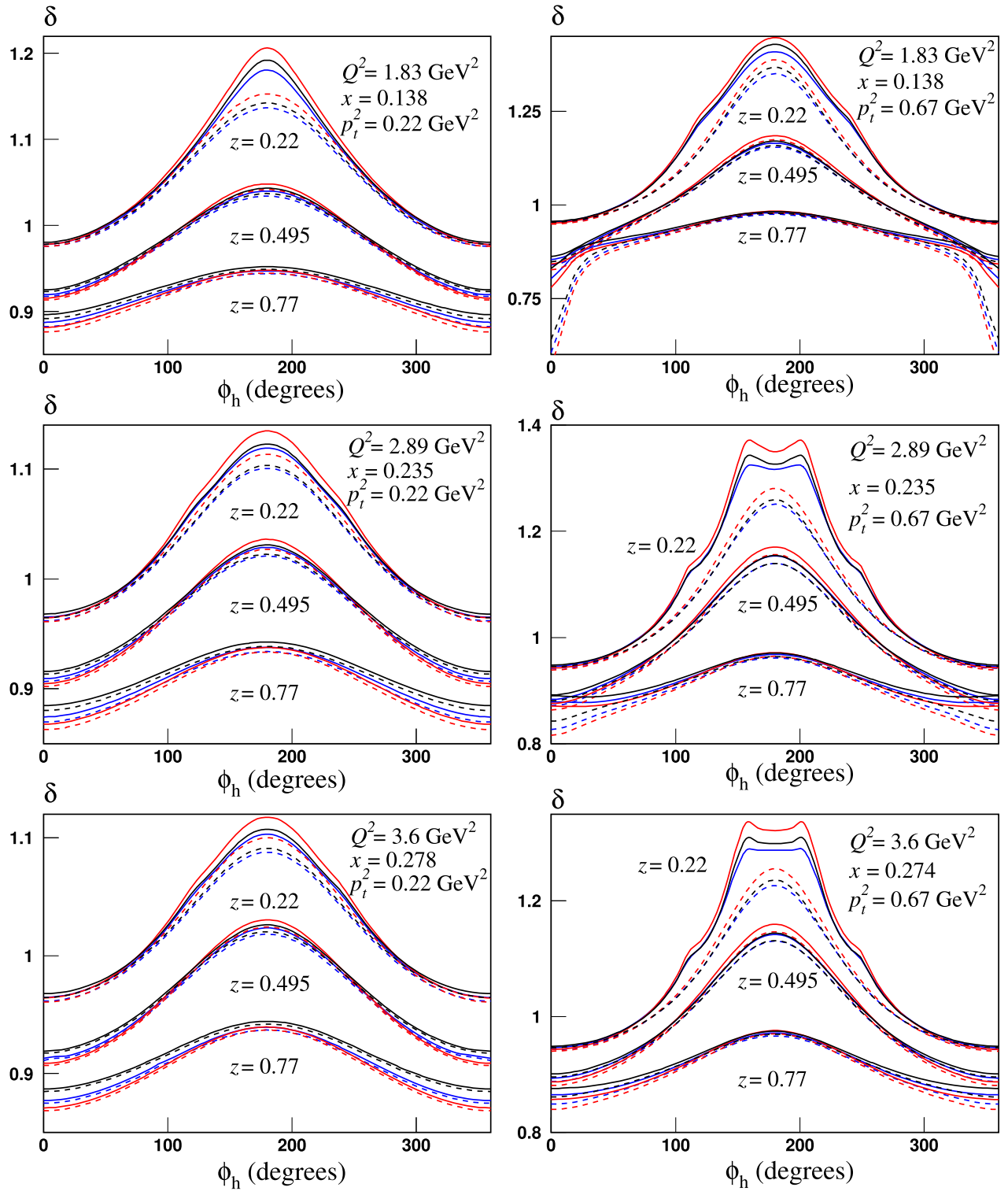
FIG. 7. The ϕ_h-dependence of the RC factor for semi-inclusive π^+ electroproduction for the lepton beam energy equal to 10.65 GeV. Solid lines show the total RC factor, and dashed lines represent the RC factor calculated excluding the exclusive radiative tail. The blue, red, and black lines show the RC factor calculated exactly, using the methods of the leading log approximation in the lowest order in respect of α and the method of the electron structure functions, respectively.

Born cross section with shifted kinematics. Traditionally, these RC include effects caused by loop corrections and soft and hard collinear radiation of photons and e^+e^- pairs. This method can be improved by including effects due to radiation of one noncollinear photon. The corresponding procedure results in a modification of the hard part of the cross section, which takes the lowest order correction into account exactly and allows going beyond the leading approximation [23].

Recently, Liu *et al.* [25] proposed a QCD-like factorization to take into account the QED RC to the experimentally measured cross sections of both inclusive and semi-inclusive lepton-nucleon DIS. This approach is similar to the approach for RC calculations involving the formalism of electron structure functions [20–23]. Since this approach is one of the three approaches we used in this paper, the resulting formula in the leading approximation (67) has to be comparable to Eq. (3.30) obtained by Liu *et al.* [25]. We note, however, that the comparison deserves some comments.

First, the lowest limits of integration in [25], $\xi_{\min}$ and $\zeta_{\min}$, are given by Eqs. (2.24a) and (2.24b) and are identical for both inclusive and semi-inclusive RC. The expressions for $\xi_{\min}$ and $\zeta_{\min}$ are calculated ignoring the restriction of the photon phase space by the pion threshold. The formulas for the lower limits of integrations z_{1m} and z_{2m} are given by Eq. (11) (and subsequent formula) of [22] for the inclusive case and Eqs. (38) and (68) in the present paper. The formulas for z_{1m} and z_{2m} are not identical for DIS and SIDIS. This is expected because they can depend on x and y for the DIS case and on all five variables (3) that describe the kinematics of the SIDIS process. These formulas for the inclusive case contain the term z_{th} and reproduce $\xi_{\min}$ and $\zeta_{\min}$ when this term tends to zero.

We believe that the pion threshold is necessary for both DIS and SIDIS RC to appropriately separate the contributions of the parts of the total RC with a single hadron and a continuum of particles in the final unobserved hadronic state. These two types of the contributions to RC require different models of hadronic structure (e.g., DIS/SIDIS structure functions for the continuum of unobserved particles and form factors for the elastic radiative tail or exclusive structure functions for the exclusive radiative tail) and different models for the phase of space of unobserved particles (a fixed invariant mass of the final hadronic state reduces the number of integrations over the photon kinematical variables by one). Ignoring the pion threshold in the formula for RC implies that the elastic radiative tail for DIS RC and exclusive RC for SIDIS RC can be obtained from the expressions for RC for the continuum of particles by their extrapolation through the pion threshold and applying the obtained approximate formulas for the RC with one hadron in the final unobserved hadronic state. This approximation is poor and is not used since the seminal paper of Mo and Tsai [2] for the calculation of RC in DIS.

Second, the expressions for the electron structure functions that are constructed and used in the formalism of the electron structure functions [20–23] are not identical to the lepton distribution and lepton fragmentation functions obtained by Liu *et al.* [25]. The standard formula for the electron structure functions, D, includes three terms presented by Eq. (69). The functions D^γ in the formalism of the electron structure functions that correspond to the initial and final state radiation are identical, but respective functions obtained and used in [25] (they are refereed as the universal lepton distribution and lepton fragmentation functions) are not due to the difference in the factor under the leading log in (2.18) and (2.20) of [25]. We note that this difference does not affect the leading log part of the total RC. Furthermore, the functions D presented in [25] are not complete because they do not include the effects of collinear electron pair production (i.e., $D_N^{e^+e^-} = 0$ and $D_S^{e^+e^-} = 0$), and the effects of multiple photon emission are presented in the lowest order only, i.e., the function D^γ contains only the term with the δ-function and the first term in the sum over k in Eq. (8) of [22].

Finally, several contributions are unavoidable when we calculate the total RC exactly or when those in the leading log approximation are not presented in the formulas of Ref. [25]. These include the elastic and exclusive radiative tails for inclusive and semi-inclusive RC (as we partly discussed above) and the effect of vacuum polarization for both processes.

The availability of both exact and leading log formulas allowed us to perform a detailed comparison of RC calculated using both approaches. We found that generally the leading log approximation gives the main contribution in the kinematics of modern JLab measurements. The factor $\log Q^2/m^2$ is of order 15 for JLab energies, so the leading log approximation provides a reasonable approximation in the broad range of kinematics. However, we also detected the regions where the next-to-leading correction cannot be avoided, e.g., at the region near $\phi_h = 180°$ and small z. The role of the next-to-leading terms is expected to be more important in the case of the polarization measurement. For asymmetries the leading log terms are (partly) factorized, so they can have a tendency for cancellation in the numerator (spin-dependent part of the cross section) and denominator (unpolarized part of the cross section).

We note that formula (1) gives an idea on how to extract the leading log results numerically using the available code for exact RC computation. We need to obtain the results for σ'_{RC} calculated for an artificial value of the electron mass nm (where n is an arbitrary value, e.g., mass nm, $n = 10$) in addition to the results calculated using the regular value of m. Since both A and B are independent of the electron mass, the value of A can be obtained as $\sigma'_{RC} - \sigma_{RC} = (\log(Q^2/n^2m^2) - \log(Q^2/m^2))A = -\log(n^2)A$. This approach provides a tool allowing us to test both leading log codes and codes that are based on the exact formulas.

APPENDIX: TREATMENT OF THE INFRARED DIVERGENCE

According to the Bardin-Shumeiko approach [1] the infrared divergence in (33) has to be extracted using an identical transformation:

$$d\sigma_{s,p}^R = d\sigma_{s,p}^R - d\sigma_{s,p}^{IR} + d\sigma_{s,p}^{IR} = d\sigma_{s,p}^F + d\sigma_{s,p}^{IR}, \quad (A1)$$

where

$$\sigma_s^F = \sigma_s^R - \sigma_s^{IR}$$
$$= \frac{\alpha}{2\pi} l_m \int\limits_{z_1^m}^{1} dz_1 \left(\frac{1+z_1^2}{1-z_1} \frac{p_{ls} S_x^2}{p_l (z_1 S - X)^2} \sigma_B(z_1 S, z_1 Q^2, x_s, z_s, p_{ts}, \cos\phi_{hs}) - \frac{2}{1-z_1} \sigma_B(S, Q^2, x, z, p_{-t}, \cos\phi_h) \right),$$

$$\sigma_p^F = \sigma_p^R - \sigma_p^{IR}$$
$$= \frac{\alpha}{2\pi} l_m \int\limits_{z_2^m}^{1} \frac{dz_2}{z_2} \left(\frac{1+z_2^2}{z_2(1-z_2)} \frac{p_{lp} S_x^2}{p_l (S - X/z_2)^2} \sigma_B(S, z_2^{-1} Q^2, x_p, z_p, p_{tp}, \cos\phi_{hp}) - \frac{2}{1-z_2} \sigma_B(S, Q^2, x, z, p_t, \cos\phi_h) \right), \quad (A3)$$

where the lowest limits of integration are defined by Eq. (38).

The remaining terms $d\sigma_{s,p}^{IR}$ are infrared divergent, so all further manipulations with them have to be performed in the dimensional regularization. Using the methods of Appendix C of [8] we obtain the resulting expressions in the leading order

$$\sigma_s^{IR} + \sigma_p^{IR} = \frac{\alpha}{\pi} \delta_{IR} \sigma_B(S, Q^2, x, z, p_t, \cos\phi_h)$$
$$= \frac{\alpha}{\pi} \left[l_m \left(2P_{IR} + 2\log\frac{m}{\nu} + \log\frac{(p_x^2 - M_{th}^2)^2}{S'X'} \right) \right.$$
$$\left. + \frac{1}{2} l_m^2 \right] \sigma_B(S, Q^2, x, z, p_t, \cos\phi_h). \quad (A4)$$

Both the infrared divergence P_{IR} term and the term containing the square of l_m cancel in the sum with the corresponding vertex contribution that can be obtained from Eq. (50) of [8] in the limit $m \to 0$:

$$\delta_{vert} = l_m \left(\frac{3}{2} - 2P_{IR} - 2\log\frac{m}{\nu} \right) - \frac{1}{2} l_m^2. \quad (A5)$$

$$d\sigma_s^{IR} = \frac{\alpha}{2\pi^2} d\sigma_B \frac{1}{(1-z_1)kk_1} \frac{d^3k}{k_0},$$
$$d\sigma_p^{IR} = \frac{\alpha}{2\pi^2} d\sigma_B \frac{z_2}{(1-z_2)kk_2} \frac{d^3k}{k_0}. \quad (A2)$$

The transformation (A1) is performed in the dimensional regularization. The terms $d\sigma_{s,p}^F$ obtained as the result of the subtraction of (A2) are infrared-free, and can be further dealt with in the regular four-dimensional space. The methods described in Sec. III A allow one to represent these terms in the form

Summing up $\sigma_{s,p}^F$ defined by Eq. (A3), $\sigma_{s,p}^{IR}$, $\alpha/\pi\delta_{vert}\sigma_B(S, Q^2, x, z, p_t, \cos\phi_h)$, and vacuum polarization $\alpha/\pi\delta_{vac}^l(Q^2)\sigma_B(S, Q^2, x, z, p_t, \cos\phi_h)$, we can find that the radiative corrected cross section in the leading approximation reads

$$\sigma_{1L}^{in} = \left[1 + \frac{\alpha}{\pi} (\delta_{VR} + \delta_{vac}^l(Q^2)) \right] \sigma_B(S, Q^2, x, z, p_t, \phi_h)$$
$$+ \sigma_s^F + \sigma_p^F, \quad (A6)$$

where

$$\delta_{VR} = \delta_{IR} + \delta_{vert} = l_m \log\frac{(p_x^2 - M_{th}^2)^2}{S'X'} + \frac{3}{2} l_m, \quad (A7)$$

and $\delta_{vac}^l(Q^2)$ is defined by Eq. (40).

The expression for σ_{1L}^{in} can be explicitly presented in terms of the splitting function (35):

$$\sigma_{1L}^{\mathrm{in}} = \left[1 + \frac{\alpha}{\pi}\delta_{\mathrm{vac}}^l(Q^2)\right]\sigma_B(S, Q^2, x, z, p_t, \phi_h) + \frac{\alpha}{2\pi}l_m\left[\int_{z_1^m}^1 dz_1 P(z_1)\frac{p_{ls}S_x^2}{p_l(z_1 S - X)^2}\sigma_B(z_1 S, z_1 Q^2, x_s, z_s, p_{ts}, \cos\phi_{hs})\right.$$

$$\left. + \int_{z_2^m}^1 dz_2 \frac{P(z_2)}{z_2^2}\frac{p_{lp}S_x^2}{p_l(S - X/z_2)^2}\sigma_B(S, Q^2/z_2, x_p, z_p, p_{tp}, \cos\phi_{hp})\right]. \tag{A8}$$

The explicit expression for $\sigma_{1L}^{\mathrm{in}}$ is given in Eq. (39).

---

[1] D. Yu. Bardin and N. M. Shumeiko, Nucl. Phys. **B127**, 242 (1977).

[2] L. W. Mo and Y.-S. Tsai, Rev. Mod. Phys. **41**, 205 (1969).

[3] A. V. Soroko and N. M. Shumeiko, Yad. Fiz. **49**, 1348 (1989) [Sov. J. Nucl. Phys. **49**, 838 (1989)].

[4] A. V. Soroko and N. M. Shumeiko, Yad. Fiz. **53**, 1015 (1991) [Sov. J. Nucl. Phys. **53**, 628 (1991)].

[5] I. Akushevich, A. Ilyichev, N. Shumeiko, A. Soroko, and A. Tolkachev, Comput. Phys. Commun. **104**, 201 (1997).

[6] I. Akushevich, N. Shumeiko, and A. Soroko, Eur. Phys. J. C **10**, 681 (1999).

[7] I. Akushevich, A. Ilyichev, and M. Osipenko, Phys. Lett. B **672**, 35 (2009).

[8] I. Akushevich and A. Ilyichev, Phys. Rev. D **100**, 033005 (2019).

[9] Y. L. Dokshitzer, Zh. Eksp. Teor. Fiz. **73**, 1216 (1977) [Sov. Phys. JETP **46**, 641 (1977)].

[10] V. N. Gribov and L. N. Lipatov, Yad. Fiz. **15**, 781 (1972) [Sov. J. Nucl. Phys. **15**, 438 (1972)].

[11] G. Altarelli and G. Parisi, Nucl. Phys. **B126**, 298 (1977).

[12] A. De Rújula, R. Petronzio, and A. Savoy-Navarro, Nucl. Phys. **B154**, 394 (1979).

[13] J. Blümlein, Z. Phys. C **47**, 89 (1990).

[14] J. Kripfganz, H. J. Mohring, and H. Spiesberger, Z. Phys. C **49**, 501 (1991).

[15] M. Skrzypek, Acta Phys. Pol. B **23**, 135 (1992).

[16] J. Blümlein and H. Kawamura, Phys. Lett. B **553**, 242 (2003).

[17] J. Blümlein and H. Kawamura, Nucl. Phys. **B708**, 467 (2005).

[18] I. Akushevich, A. Ilyichev, and N. M. Shumeiko, Phys. Rev. D **90**, 033001 (2014).

[19] I. Akushevich and A. Ilyichev, Phys. Rev. D **98**, 013005 (2018).

[20] E. A. Kuraev and V. S. Fadin, Yad. Fiz. **41**, 733 (1985) [Sov. J. Nucl. Phys. **41**, 466 (1985)].

[21] E. A. Kuraev, N. P. Merenkov, and V. S. Fadin, Yad. Fiz. **47**, 1593 (1988) [Sov. J. Nucl. Phys. **47**, 1009 (1988)].

[22] A. V. Afanasev, I. Akushevich, and N. P. Merenkov, J. Exp. Theor. Phys. **98**, 403 (2004).

[23] A. Afanasev, I. Akushevich, A. Ilyichev, and N. Merenkov, in *Proceedings of the 17th International Workshop on High-Energy Physics and Quantum Field Theory (QFTHEP 2003)* (2003), pp. 154–161, arXiv:2212.04730.

[24] S. Frixione, E. Laenen, C. Calame, A. Denner, S. Dittmaier, T. Engel, L. Flower, L. Gellersen, S. Hoeche, S. Jadach *et al.*, arXiv:2203.12557.

[25] T. Liu, W. Melnitchouk, J.-W. Qiu, and N. Sato, J. High Energy Phys. 11 (2021) 157.

[26] A. Bacchetta, M. Diehl, K. Goeke, A. Metz, P. J. Mulders, and M. Schlegel, J. High Energy Phys. 02 (2007) 093.

[27] I. Akushevich and A. Ilyichev, Phys. Rev. D **85**, 053008 (2012).

[28] I. V. Akushevich, A. N. Ilichev, and N. M. Shumeiko, Yad. Fiz. **61**, 2268 (1998) [Sov. J. Nucl. Phys. **61**, 2154 (1998)].

[29] S. Jadach, M. Skrzypek, and B. F. L. Ward, Phys. Rev. D **47**, 3733 (1993).

[30] A. Afanasev, I. Akushevich, V. Burkert, and K. Joo, Phys. Rev. D **66**, 074004 (2002).

[31] S. Bastami *et al.*, J. High Energy Phys. 06 (2019) 007.

[32] https://maid.kph.uni-mainz.de/maid2007/maid2007.html.